Dynamics of the Oocyte Cortical Cytoskeleton During Oogenesis

by

Sandra Maria Graham McPherson

A Thesis

presented to the University of Manitoba

in partial fulfillment of the

requirements for the degree of

Masters of Science

in Zoology

Winnipeg, Manitoba

ISBN 0-315-51644-5

DYNAMICS OF THE OOCYTE CORTICAL CYTOSKELETON DURING OOGENESIS

BY

SANDRA MARIA GRAHAM McPHERSON

A thesis submitted to the Faculty of Graduate Studies of the University of Manitoba in partial fulfillment of the requirements of the degree of

MASTER OF SCIENCE

I hereby declare that I am the sole author of this thesis.

Sandra McPherson

I authorize the University of Manitoba to reproduce this thesis by photocopying or by other means, in total or in part, at the request of other institutions or individuals for the purpose of scholarly research.

Sandra McPherson

ABSTRACT

The oocyte cortex undergoes dramatic changes during oogenesis in Rhodnius prolixus. Despite numerous studies examining oogenesis in the telotrophic ovariole, none have investigated the ultrastructural details of the oocyte cortex, in particular, the lateral cortical cytoskeleton. In this study I describe the dynamics of the oocyte cortex from early previtellogenesis to late vitellogenesis using indirect immunofluorescence and rhodamine phalloidin staining in conjunction with transmission and scanning electron microscopy.

During early previtellogenesis, oocytes 50-150 uM in length have a smooth oolemma, and there does not appear to be a discernible cortical cytoskeleton. During mid to late previtellogenesis, 150-350 uM in length, a tightly woven network of microfilaments and microtubules has formed, excluding mitochondria and Golgi complexes from the lateral cortex. Throughout the late stages of previtellogenesis I found a novel configuration of rough endoplasmic reticulum packaging in the deep cortex. The cisternae are linked by what appears to be a fibrous material so that they form large whorls.

At the onset of vitellogenesis, the follicle becomes patent, and there is an increase in microvilli covering the lateral oocyte surface. The microfilament cores form a discrete pattern that corresponds to the imprint of the follicle cells on the oocyte surface. While the lateral microfilament cytoskeleton becomes more elaborate, the lateral microtubule cytoskeleton diminishes, remaining sparse throughout vitellogenesis.

The oocyte cortical cytoskeleton undergoes dramatic changes during oogenesis that are visualized by a variety of techniques. These dynamics are intricately related to the cellular and molecular processes that occur during oogenesis.

ACKNOWLWDGEMENTS

I would like to thank Dr. Erwin Huebner for sharing his wisdom and friendship with me during the past few years. I would also like to thank my lab partners Bill Diehl-Jones, Greg Kelly and Gunnar Valdimarsson for their friendship and for countless discussions on a great variety of topics. I would like to acknowledge the members of my committee, Dr. J. Gerrard and Dr. M. Sumner for their time and critical appraisal of this thesis. I would like to thank Mr. B. Liut for operating the scanning electron microscope and Dr. J. Cheung, Agriculture Canada, for allowing me use of their Transmission Electron Microscope. I would like to acknowledge financial assistance from a University of Manitoba Fellowship, a Canadian Society of Entomology Scholarship, and a Natural Sciences and Engineering Postgraduate Scholarship.

I would like to thank Bill and Charlene Diehl-Jones for welcoming me into their home and family while I was writing this thesis. Their friendship is greatly valued.

I would like to thank my parents, Neil and Maria Graham and my sisters Susan and Janet for their support and encouragement throughout the course of this work

and beyond. Finally, I thank my husband Peter McPherson for his endless enthusiasm and for his confidence in me and this thesis. His encouragement was an important part of this work.

TABLE OF CONTENTS

INTRODUCTION

Oogenesis is an intricate process resulting in a cell endowed with a variety of features. The growing oocytes must be sustained and accumulate and store all the materials and information necessary for fertilization and early embryogenesis (Wilson, 1925; Schatten, 1982; Sardet and Chang, 1987). The oocyte cortex has an important role in the growth of the unfertilized egg and in the development of the early embryo (for reviews see Raven, 1970; Burgess and Schroeder, 1979; Vacquier, 1981; Longo, 1985 and Sardet and Chang, 1987). "Classically this region, (the cortex) is shown to be associated with determinants that specify the future of embryonic cells and limit their potential early in development long before the cells in question manifest their fate" (Davidson, 1980 in Longo, 1985). The term cortex has been ascribed to varying parts of the cell periphery (Sardet and Chang, 1987). For my thesis the cortex is best defined as the layer of cytoplasm (and the included organelles) beneath and including the plasma membrane that is functionally and structurally different from the underlying cytoplasm (Ben Ze'ev, Duerr, Solomon, and

Penman, 1979 in Tucker, 1981 and Sardet and Chang, 1987). Cytoskeletal proteins are important components of the oocyte cortex. There are three major types of cytoskeletal elements: microtubules, microfilaments and intermediate filaments. These elements are responsible for many functions; such as the formation of a fertilization cone (Longo, 1980), the contractile force needed for cleavage (Schroeder, 1972 and 1973) and for polar body formation (Sardet and Chang, 1987) among others. Even in the echinoderms where the cortex has been best studied there is still much to be discovered about its regional morphology and role in development (Wang and Taylor, 1979; Longo, 1980 & 1986; Schatten and Schatten, 1983; Chandler and Heuser, 1981; Schroeder and Stricker, 1983; Otto and Schroeder, 1984b; Yonemura and Kinoshita, 1986 and Henson and Begg, 1988. The cortex of oocytes and embryos of other groups have been the subject of relatively few studies. For example amphibians (Franke et al., 1976; Elinson and Manes, 1978 and Colombo et al., 1981), and annelids (Shimizu, 1986 and 1988), ascidians (Satoh and Deno, 1980 and Sawada and Osnai, 1985), molluscs (Speksnijder et al, 1986 and Huebner and Dohmen, 1988) and mammalian (Shagli and Phillips, 1980). Insects provide a good

system to investigate how the cortex develops in oocytes. The telotrophic ovary, in particular, with its relatively large eggs, undergoes a variety of complex changes which make it an excellent choice for the study of the oocyte cortex. The ovariole presents an excellent model with which to study basic cellular processes such as, organelle transport, receptor mediated endocytosis, nuclear migration, interaction of cytoskeletal elements with each other, with organelles (mitochondria, clathrin coated vesicles, nuclei and mRNA) and with the plasma membrane. Although there have been many microscopical studies on the telotrophic ovary, none have looked at the dynamics of the oocyte cortex, particularly the cytoskeleton (Bonhag, 1955; Vanderberg, 1963; Hopkins and King, 1966 and Schreiner, 1977). The oolemma undergoes changes in concert with the dynamic restructuring of the follicular epithelium. There is an abundance of knowledge, both ultrastructural and physiological, of the events of oogenesis in the telotrophic ovary of Rhodnius prolixus. Thus, it provides a good model system to relate the development of the cortex and its changes relative to the differentiation of the oocyte.

The structure of the meroistic telotrophic ovary has been well documented (see Bonhag, 1955; Huebner and Injeyan, 1981; Huebner and Anderson, 1972a, b & c and Huebner, 1984). However, reiteration of the relevant aspects provide a useful background for this study. There are two ovaries, each composed of seven ovarioles. The ovariole is divided into two distinct regions, the tropharium and the vitellarium. The upper tropharium houses a syncytium of nurse cells connected via intercellular bridges the result of incomplete cytokinesis (Huebner, 1984). The nurse cells synthesize messenger and ribosomal RNA, proteins and mitochondria (Vanderberg, 1963; Telfer, 1975 and Huebner, 1984). These materials are transported into a microtubule packed trophic core and down the trophic cords that lead to individual oocytes (MacGregor and Stebbings, 1970, Huebner, 1984 and Valdimarsson and Huebner, 1989). The oocytes remain attached to the nurse cells until mid- vitellogenesis. Oocytes are arrested in meiotic prophase I (diplotene) throughout oogenesis, and are found in developmental succession in the vitellarium (Huebner and Anderson, 1972b). Oocytes in a quiescent stage, 20 to 100uM in length, lie at the base of the tropharium surrounded by prefollicular

tissue (Huebner, 1984). Once the oocyte begins previtellogenic growth, 100 to 200uM in length, it enlarges due to accumulation of materials from the nurse cells. It moves further away from the base of the tropharium and at the same time the prefollicular tissue differentiates into a follicular epithelium (Huebner, 1984). During this previtellogenic growth, the oocyte nucleus (germinal vesicle) occupies a central position in the ooplasm. By late previtellogenesis, 350 to 400uM in length, it has migrated to the lateral cortex (Huebner and Anderson, 1972b). Throughout oogenesis, the germinal vesicle is thought to be inactive or at a low level of synthesis, the majority of synthetic activity occurs in the nurse cells (Huebner, 1984). During previtellogenic growth the oocyte must synthesize or accumulate the necessary macromolecules that are essential for the development of a plasma membrane and cortical components capable of initiating and sustaining pinocytotic uptake of yolk precursors during vitellogenesis. Examples of such components include clathrin, surface receptors and cytoskeletal elements. At the onset of vitellogenesis which is the uptake of yolk precursors from the hemolymph, oocytes are 400 to 500uM in length, the

follicle becomes patent, the lateral follicle cells separate forming intercellular spaces rich in yolk precursors between themselves and the oocyte. The anterior and posterior follicle cells do not separate. This correlates with a lack or reduction of pinocytotic activity in the adjacent oolemma.

During vitellogenesis the oocyte increases in size rapidly with the accumulation of yolk centrally and a thin rim of cytoplasm at the periphery. There is only one vitellogenic follicle per ovariole, the others remain in various stages of previtellogenesis. Once the oocyte has reached approximately 1600uM vitellogenesis is complete. The lateral follicle cells then undergo dramatic cytoskeletal changes in order to close the inter-spaces, and begin secreting the acellular chorion (Huebner, 1984 and Watson and Huebner, 1986).

Microtubules are generally relatively rare in growing oocytes. Polymerized tubulin is not found in sea urchin oocytes until after fertilization (Harris et al, 1980; Bestor and Schatten, 1981 and Foucault et al, 1987). Because of this there was little reason to think otherwise for oocytes of other species (Otto and Schroeder, 1984a). However, recently microtubules have

been found in the oocytes of the annelid Tubifex (Shimizu, 1981), the sea snail Lymnaea (Morrill and Perkins, 1973 and Otto & Schroeder, 1984a), the amphibian Xenopus (Heidemann et al, 1985; Palecek et al, 1985; Lessman, 1987 and Jessus et al, 1987), the starfish Pisaster ochrceus, the surf clam Spisula and the oocytes of the sturgeon (Otto and Schroeder, 1984a and Schroeder and Otto, 1984).

Microtubules are the largest of the cytoskeletal elements. They are 20 to 25nM in diameter and are composed of heterodimers, one and one tubulin, each of equal molecular weight (Cleveland, 1983). Microtubules are polar, they have a plus and a minus end. Polymerization of subunits occurs at the plus end, while disassembly occurs at the minus end (Bergen and Borisy, 1980). Microtubules are involved in the maintenance of cell shape (Handel and Roth, 1971, Osborn and Weber, 1977 and Wolosewick and Porter, 1979); intracellular transport (Cleveland, 1983; Hayden and Allen, 1984 and Stebbings, 1986); they are the major components of the mitotic and meiotic spindles (Mahowald, 1972 and Cleveland, 1983); and they have been observed associated with coated vesicles (Imhof et al, 1983). Microtubules in the oocytes of Rana pipiens

and Xenopus maintain the position of the germinal vesicle until it migrates to the oocyte cortex (Dumont and Wallace, 1972; Colman et al, 1981; Heidemann et al, 1985; Jessus et al, 1986 and Lessman, 1987). Microtubules are also implicated in the movement of mitochondria (Huebner and Anderson, 1970; Ducibella et al, 1977; Heggeness et al, 1978; Johnson et al, 1980 and Stebbings, 1986).

Actin, is the major cytoskeletal protein found in the cortices of unfertilized eggs (Vacquier, 1981; Sardet, 1984; Sardet and Chang, 1987 and Longo, 1987). Longo (1987) has found using gel densitometry that actin makes up approximately 2% of the total protein in both eggs and oocytes of sea urchins. Most of this actin in the sea urchin oocytes, is in the monomeric form, G-actin (Burgess, 1977 and Spudich and Spudich, 1979). This was encouraged by early transmission electron microscopy studies which failed to reveal many filaments in the unfertilized sea urchin egg (Longo, 1980; Coffe et al, 1982 and Henson and Begg, 1988). However, more recent studies using improved methods of staining and preservation have shown the presence of microfilaments in sea urchin oocyte cortices (Henson and Begg, 1988). Rhodamine phalloidin staining of F-

actin (Wieland, 1977 in Yonemura and Kinoshita, 1986) has revealed weak staining in the cortical regions of the sand dollar oocyte (Yonemura and Kinoshita, 1986).

Microfilaments are composed of actin monomers which have a molecular weight of approximately 42kD (Korn, 1982). The cytoplasmic actins are the and type. Microfilaments are about 5nM in diameter and their functioning in vivo is dependent upon their interaction with the various types of actin binding proteins present (Weeds, 1982; Mooseker, 1983; Stossel, 1984 and Harris, 1987). Microfilaments have been described in the unfertilized amphibian egg (Franke et al, 1976) and they form the filamentous core of microvilli in the oocyte of the sea anemone Tealia crassicornis (Schroeder, 1982) and in the microvilli of the fertilized sea urchin egg (Spudich and Amos, 1979). Microfilaments are implicated in the movement of mitochondria in fertilized Tubifex eggs (Shimizu, 1985) and in the migration of the germinal vesicle in the oocytes of Xenopus (Lessman, 1987). They are also the major component of the contractile ring (Schroeder, 1972 and 1973). Sardet (1984) has observed microfilaments "on the inside face of the plasma membrane running in between microvilli and connecting

organelles to the plasma membrane".

Intermediate filaments are a relatively new group of proteins, they were first described in 1969 (Lazarides, 1980 and Godsave, 1984a). They are approximately 10nM in diameter and are resistent to high salt buffers and Triton X-100 extraction (Franke et al, 1978; Lazarides, 1980 and Franz et al, 1983). Intermediate filaments are divided into five major groups: keratin -found in epithelial cells, desmin - found in muscle cells, vimentin -found in mesenchymal cells and cells of mesenchymal origin, neurofilaments - found in neurons, and glial filaments -found in all types of glial cells (Lazarides, 1980 and Steinert et al, 1984). Intermediate filaments are thought to have a structural role, mechanical support, due to their insolubility in high salt buffers (Lazarides, 1980 and Godsave et al, 1984b). Vimentin forms an intricate network around the nucleus, possibly maintaining its position (Lazarides, 1980). It was previously thought that germ cells did not contain intermediate filaments of any type (Jackson et al, 1980). However, Virtanen et al (1984) have discovered a band of vimentin filaments that runs around the head of human sperm and other researchers (Franz et al, 1983; Gall et al, 1983;

Godsave et al, 1984a & b and Klymkowsky et al, 1987) have found a "highly organized network of cytokeratin filaments and vimentin in the oocytes of Xenopus laevis".

There has been a proliferation of literature on the study of messenger RNA and its association with the cytoskeleton, specifically intermediate filaments, and the implications of such an association (Lenk et al, 1977; Lenk and Penman, 1979; Moon et al, 1983; Jeffery, 1983; Howe and Hershey, 1984; Jeffery et al, 1986 and Bag and Pramanik, 1987). Capco and Jeffery (1979) probed the distribution of poly(A)+[RNA] in the telotrophic ovariole of Oncopeltus using in situ hybridization. They found high binding of label over the nurse and follicle cells. The label was uniformly distributed over the ooplasm until late vitellogenesis, at which time it was localized to the anterior and posterior cortical regions more so than in the lateral cortex (Capco and Jeffery, 1979).

Watson and Huebner (1986) showed a correlation between the dynamics of the follicle cell cytoskeleton and the follicle cell shape in Rhodnius prolixus. It then follows that the oocyte cytoskeleton may influence the oocyte shape. Thus, the major objectives of my

study of the Rhodnius oocyte are to (1) to examine the cortex and determine the structural changes that occur during oogenesis, (2) to identify the cytoskeletal components and their organization into a cortical cytoskeleton, (3) to correlate changes in the cortex with the dynamics of the cytoskeleton.

The methods of study were chosen so that I could observe the cortex structure in a condition as close as possible to the in vivo situation. The use of any one of the following techniques alone would result in an insufficient and possibly inaccurate analysis of the oocyte cortex. Indirect immunofluorescence of sections is a common method used to view the overall network of cytoskeletal filaments in a cell (Weber et al, 1975; Weber et al, 1978; Weber and Osborn, 1979 and Otto and Schroeder, 1984a, b). Indirect immuno- fluorescence of sections embedded in diethylene glycol disterate (DGD) was carried out as per Valdimarsson and Huebner (1989). DGD offers good preservation of cellular structure and is easily removed without exposure to extremely harsh conditions (Valdimarsson and Huebner, 1989). The Anti-Tubulin antibody was raised against tubulin and therefore binds not only microtubules but also the tubulin subunits. This is also the case for the Anti-

Actin antibody. This method then presents a good avenue to study overall distribution of polymerized and nonpolymerized proteins. Scanning electron microscopy of denuded oocytes allows one to examine the 3-dimensional details of oolemma modifications (Eddy and Shapiro, 1976 and Villa and Patricola, 1987). However, while it permits general visualization of the cytoskeleton it does not allow for the positive identification of specific cytoskeletal elements. These two methods were complemented by transmission electron microscopy (TEM), to reveal and identify the presence of cytoskeletal elements and provide ultra-structural detail of their organization in the cortex. Rhodamine phalloidin staining of F-actin allows for a general overview characterization of the actin distribution in the entire oocyte which is not easily possible in a TEM thin section. Preliminary studies to localize intermediate filaments were also attempted as well as the localization of poly(A)+[RNA] to determine if mRNA is localized in the cortex. Messenger RNAs were initially referred to as 'cytoplasmic determinants', the factors which caused the embryo to develop by a set pattern (Davidson, 1986 and Gilbert, 1988). In insects the early embryo forms a syncytial

blastoderm, that is the cell undergoes extensive nuclear division, these nuclei then migrate to the cortex. " In insects the pattern of future body is not predetermined in the ooplasm by a detailed mosaic of localized determinants. The embryonic pattern can be altered in a global way during the period between egg deposition and the blastoderm or germ band stages" (Zissler & Sander, 1982). The study of cytoplasmic mRNA localization, masking and gradient formation and possible involvement of the cytoskeleton in transcription regulation in the oocyte may aid in the elucidation of embryonic development.

MATERIALS AND METHODS

Animal Rearing Techniques

A colony of Rhodnius prolixus (Stahl) was kept in a controlled environment at high humidity and 27°C according to the methods of Huebner and Anderson 1972a). The colony was fed at four week intervals on female New Zealand white rabbits. Mated adult females were dissected in Rhodnius saline containing 129.0mM NaCl, 8.6mM KCl, 2.0mM$CaCl_2$, 8.5mMMgCl_2, 4.3mMNaH_2PO_4, 10.3mM $NaHCO_3$ and 34.0mM glucose (Maddrell, 1969) or in O'Donnell ringers (O'Donnell, 1986) two to four days post- feed to obtain the various stages of oocytes. Oocytes were examined in the resting stage, 20 to 100uM in length; previtellogenesis 100 to 350uM; early vitellogenesis, 400 to 800uM; and late vitellogenesis, 800 to 1600uM.

Scanning Electron Microscopy

Ovarioles were desheathed in a microfilament (MF) stabilization buffer [80mM KCl, 20mM piperazine-N, N'-bis 2-ethanesulfonic acid (PIPES), 1.5mM $MgCl_2$, 10mM

ethyleneglycol-bis-(-aminethyl ether)-N, N, N', N'-tetraacetic acid (EGTA), 5.6mM dextrose, and 1.2 to 1.5mM $CaCl_2$] (Bond and Somylo, 1982) containing 10mM p-Tosyl-L-Arginine methyl ester (TAME) (Kane, 1986). Proteolytic digestion, 3-5 min in 0.5% protease in MF buffer plus 10mM TAME and three washes in MF buffer plus 10mM TAME preceded mechanical removal of the basal lamina with an electrolytically sharpened tungsten needle (Juurlink and Dell, 1980). Some ovarioles were then placed in 0.1% Triton X-100 (or 30% glycerol) in MF buffer plus 10mM TAME, while others were left unextracted. During the extraction of approximately 25 min, the tissue was placed on a KOH cleaned poly-L-lysine (Mw. 183,000-271,000, Sigma Chem Co.) coated coverslip (Mazia et al, 1975). Oocytes were denuded by rolling the follicle on the coverslip thereby peeling away follicle cells which remain attached to the glass. The tissue was washed three times in MF buffer plus 10mM TAME post- extraction. Some tissue, both extracted and unextracted, was left intact, that is with the follicle cells. Tissue was fixed for 25 to 30 min in modified Karnovsky's fixative at 4°C (Karnovsky, 1965). Following a brief wash in 0.1M sodium cacodylate buffer, pH 7.2, ovarioles were osmicated

(0.5% OsO_4 in 0.1M sodium cacodylate buffer pH 7.2) for 15 min at 4°C. The tissue was then rapidly dehydrated through an ascending series of ice cold ethyl alcohol to absolute ethyl alcohol. Ovarioles were then cleared through an ascending series of acetone in ethyl alcohol to pure acetone. Samples were critical point dried according to the Sorval CP Drier Manual. Samples left unextracted were critical point dried then cracked open with a dissecting needle and mounted. Samples were then mounted on stubs using double sided sticky tape, gold coated and examined using a Cambridge Stereo Scanning Electron Microscope.

Indirect Immunofluorescence

Indirect immunofluorescence methods were modified from Capco et al (1984), Capco and McGaughey (1986) and Valdimarsson and Huebner (1989). Ovarioles were desheathed in Rhodnius saline (Maddrell, 1969), and fixed for 30 min in 3% paraformaldehyde and 0.5% glutaraldehyde in PHEM buffer (60mM PIPES, 25mM N-2-hydroxyethylpiperazine-N'-2 ethanesulfonic acid [HEPES], 10mM EGTA and 2mM $MgCl_2$) containing 1mM GTP added just before use. Samples were then washed in

PHEM buffer plus 1mM GTP and rapidly dehydrated through an ascending series of ice cold ethyl alcohol to absolute ethyl alcohol. The tissue was then cleared through an ascending of n-butyl alcohol and infiltrated through an ascending series of molten diethylene glycol distearate (DGD) (Mw 639.0, Polysciences Inc.) in n-butyl alcohol to pure DGD containing 0.5% dimethylsulfoxide (DMSO). The samples were left in the pure DGD plus 0.5% DMSO overnight at 55-60°C. Samples were put into fresh DGD plus 0.5% DMSO for 1 hr at 55-60°C and then embedded in DGD plus 0.5% DMSO and left to harden at room temperature.

Sections (0.5 - 1uM) were cut on glass knives at a 4° angle using a Sorvall Porter-Blum MT2-B Ultramicrotome. The sections were floated onto a KOH cleaned coverslip coated with 0.5% w/v poly-L-lysine (Mw 183,000-271,000, Sigma Chem. Co.). The coverslips with the sections were dried at 55-60°C and then sections covered with glycerol and left at room temperature until the staining procedure.

DGD was removed using four 1 hr changes of n-butyl alcohol. Sections were then rehydrated through 3 min changes in 70:30, 50:50, and 30:70 solutions of n-butyl alcohol and 100% ethyl alcohol. This was followed by 3

min changes in each of 95% and 70% ethyl alcohol and a 10 min treatment in 1mg/ml $NaBH_4$ in 70% ethyl alcohol. This treatment reduces background fluorescence (Weber et al, 1978). This was followed by 3 min changes in 70% and 50% ethyl alcohol, and Dulbeccos phosphate buffered saline (PBS) (4.0g NaCl, 0.1g KCl, 1.45g $Na_2HPO_4.12H_2O$, 0.1g KH_2PO_4, 0.066g $CaCl_2.2H_2O$ and 0.05g $MgCl_2.6H_2O$ in 500mL H_2O, pH 7.2). Coverslips were then incubated with 1% BSA (Bovine Albumin Fraction V 96-99%, Sigma Chem. Co.) in Dulbeccos PBS pH 7.2 for 1 hr at 37°C in a moist light-tight chamber. This was followed by incubation at 37°C with the appropriate antibodies. A Polysciences Anti-sea urchin tubulin at 1:75 dilution and Anti-chicken gizzard actin at a 1:10 dilution were used. Various intermediate filament antibodies were also tried: Anti-IF courtesy of J. Venuti, University of Texas at Austin (Pruss et al, 1981), the sera was not diluted; Anti-*Drosophila* vimentin from H. Biessmann and M. Walter at a 1:1 dilution (University of California at Irvine) (Walter and Biessmann, 1984 and Schatten et al, 1987), and three monoclonal antibodies from N. Marceau (Laval University) 4G7, 3D1 and 4B7 (all at a 1:100 dilution) (Katsuma et al, 1987). After a 1 hr incubation with

the primary antibody, sections were subjected to three 5 min washes in 1% BSA in PBS pH 7.2 at 37°C. This was followed by incubation with the appropriate secondary antibody, either a fluorescein conjugated goat anti-rabbit or goat anti-mouse antibody (Polysciences Inc.). Control sections were not incubated in the primary antibody, with the rest of the procedure being the same.

Coverslips were then washed extensively with Dulbeccos PBS to remove any unbound label. Coverslips were mounted on glass slides in PBS and examined with epi-fluorescence microscopy on a Zeiss Photomicroscope II. Sections were photographed with Kodak Tri-X film, ASA 400. Film was developed in Acufine Developer according to the manufacturer's specifications (Acufine Inc., Chicago, Illinois).

Rhodamine Phalloidin Staining of F-Actin

Ovarioles were desheathed in a microfilament (MF) buffer (Bond and Somlyo, 1982) containing 10mM TAME (Kane, 1986). The basal lamina and the follicle cells were removed as described earlier for Scanning Electron Microscopy. Denuded oocytes were washed in MF buffer

plus 10mM TAME, and fixed for 10 min at 4°C in 8% paraformaldehyde in PBS (8.5g NaCl, 0.36g KH_2PO_4 and 3.72g Na_2HPO_4 per litre) at pH 7.0. Following three 5 min washes in PBS, ovarioles were incubated for 20 min at 25°C in rhodaminyl conjugated phalloidin (from Th. Wieland, Heidelberg) 5ug/mL in PBS (Warn et al, 1985 and Gutzeit and Huebner, 1986). The samples were then washed extensively with PBS, mounted in glycerol, and examined using epi-fluorescence microscopy on a Zeiss Photomicroscope II. Specimens were photographed with Kodak Tri-X film, ASA 400. The film was developed in Acufine Developer as specified by the manufacturer (Acufine Inc., Chicago, Illinois).

Transmission Electron Microscopy

Ovarioles were desheathed in Rhodnius saline (Maddrell, 1969). Tissue was the placed in modified Karnovsky's fixative for 0.5hr at 4°C. (Karnovsky, 1965) (0.5% w/v tannic acid and 0.5% w/v saponin was added for some specimens). Samples were then washed in 0.1M sodium cacodylate pH 7.2 for 0.5 hr at 4°C, followed by osmication (1% OsO_4 in 0.1M sodium cacodylate buffer pH 7.2) for 15 min at room

temperature. The ovarioles were then rapidly dehydrated through an ascending series of ice-cold ethyl alcohol through to absolute ethyl alcohol. Samples were equilibrated in four 0.5 hr changes of 100% ethyl alcohol at room temperature. Tissue was then exposed to a 1:1 mixture of absolute ethyl alcohol and propylene oxide for 0.25 hr, then to pure propylene for two 0.25 hr changes. Samples were then infiltrated in a 1:1 solution of propylene oxide and Epon-Araldite embedding mixture (Anderson and Ellis, 1965) for 1 hr with the cap on the vial, then overnight without the cap in the fumehood. Samples were embedded in fresh degassed Epon-Araldite embedding mixture in flat molds and placed in the oven at 55-60°C for 2-3 days.

Silver sections were cut on a Sorvall Porter Blum MT2-B Ultramicrotome with glass knives at a 4° angle. Sections were attached to copper grids, 200 mesh. Sections were stained in uranyl acetate in 50% ethyl alcohol for 0.5 hr, then rinsed in 50% ethyl alcohol. Once dry, sections were stained for 1.5 min in lead citrate (Reynolds, 1963). Sections were examined on a Philips EM 420, 60KV.

Bright Field Microscopy

Conventional brightfield microscopy was done on 0.5-1uM epoxy sections (prepared as in TEM section). Sections were placed on a clean glass slide and heated attached. The sections were stained in a 1.0% w/v toluidine blue, 1.0% w/v sodium borax solution. The sections were mounted in immersion oil and photographed on a Zeiss Photomicroscope II using Kodak Panatomic-X film at ASA 32. The film was developed in Acufine Developer (Acufine Inc., Chicago, Illinois).

In Situ Hybridization

Since the results from these experiments were not included in this thesis, only a brief description of methods will be included in this section. The complete in situ hybridization procedure can be found in Appendix I.

Desheathed ovarioles were fixed in Carnoy's fixative for 0.5 hr. The tissue was then prepared for DGD infiltration and embedding as per immunofluorescence. All slides were hybridized to ^{3}H-poly U probe for 3-4 hr at 50°C. Slides were coated

with Kodak autoradiography emulsion and exposed for 5 weeks at 4°C. Slides were developed in D-19 Kodak developer, left to dry and mounted in Permount. Sections were photographed using Kodak Technical Pan 2415 film, ASA 50.

SDS Polyacrylamide Gel Electrophoresis (PAGE)

Approximately 140 ovarioles were desheathed in Rhodnius saline (Maddrell, 1969), and homogenized in 200uL PEM buffer (PIPES, EGTA and $MgCl_2$). To this 200uL of 2x Laemmli buffer (9:1 with -mercaptoethanol) was added. This mixture was then boiled for 2 min and then centrifuged for 2 min. This mixture was then frozen at -20°C until needed. Protein content was determined by a Bradford Assay (BioRad).

PAGE was carried out according to Laemmli in a SDS discontinuous system. The apparatus used was the Protean II Cell (BioRad) and an LKB Bromma 2197 power supply. The separating gel (12.5%) contained 30% acrylamide, 1% bis-acrylamide, 1.5M Tris HCl pH 8.8, 10% SDS (w/v), 2.7% (w/v) N, N, N′, N′-tetranethylethylenediamine (TEMED) and 10% ammonium persulfate (APS) (w/v). The 5% stacking gel contained

30% acrylamide, 1% bis-acrylamide, 1M TrisHCl pH 6.8, 10% SDS, 1/100 vol 10% APS and 1/1000 vol TEMED. The tank buffer for both the upper and lower chambers was 0.025M Tris pH 8.3, 0.192M glycine and 0.1% SDS. The lower buffer was reused five times, while the upper buffer was used only once. The gel was run at 200V while in the stacking gel and at 300V while in the separating gel at 5-10°C for 4 hr.

For silver staining the gel was placed in 50% methanol for fixation overnight. The gel was placed in deionized distilled water for 30 min followed by 30 min in 5ug/mL dithiothreitol (DTT). The gel was then stained in 1% $AgNO_3$ for 30 min. A quick rinse in deionized distilled water was followed by a quick rinse in developer (15g $NaCO_3$, 500mL ddH_2O, 250uL formaldehyde). The gel was then developed over a light box. Development was arrested by the addition of 30mL of 2.3M citric acid (14.5g/30mL ddH_2O). The gel was then placed in distilled to be photographed.

Western Blotting

Once the gel was removed from the PAGE apparatus, it was equilibrated in pre-cooled blotting (transfer)

buffer containing 25mM Tris pH 8.3, 192mM glycine and 20% methanol. The nitrocellulose (NC) paper was wet slowly in the blotting buffer. The blotting procedure was carried out at 5°C, 70V for 2.5 hr. The tank buffer was the blotting buffer plus 10% SDS w/v.

Once the transfer was complete, the NC was placed in a Zip-lock bag with Blotto (0.011M $Na_2H_2PO_4.7H_2O$ and 0.15M NaCl) containing 5% w/v skim milk powder. After 12 hr, the NC was incubated with the appropriate primary antibody in Blotto plus 5% w/v skim milk powder for 6 hr. The primary antibodies used were Polysciences Anti-chicken gizzard actin (1:200 dilution), Anti-*Drosophila* vimentin (1:200 dilution, Walter and Biessmann, 1984, courtesy of Drs. H. Biessmann & M. Walter, University of California at Irvine), Anti-intermediate filament 4G7 (1:1000), 3D1 (1:1000) and 4B7 (1:1000) (from N. Marceau, Laval University, Katsuma *et al*, 1987), and Anti-IF sera courtesy of J. Venuti, Austin (Pruss *et al*, 1981). This incubation was followed by three 30 min washes in Blotto plus 5% w/v skim milk powder. After a quick rinse in Blotto (no milk), the NC sheet was incubated in TBST (1.211g Tris, 8.766g NaCl, 0.5mL Tween 20 per litre distilled water) for three 15 min changes.

Subsequently the NC sheet was incubated in the appropriate secondary antibody, either Goat Anti-mouse or Anti-rabbit alkaline phosphate conjugate (1:7,500 dilution in TBST, Promega Protoblot) for 2 hr. After three 10 min washes in TBST, the developer (10mL APS buffer and 66uL Nitro-blue tetrazolium substrate mix plus 33uL 5-bromo-4-chloro-3-indolyl phosphate) was added. Development was stopped by the addition of distilled water. Both the gels and the NC sheets were photographed using Kodak Panatomic-X film and developed in Acufine Developer (Acufine Inc., Chicago, Illinois).

RESULTS

GENERAL FEATURES OF THE OOCYTE CORTEX

The telotrophic ovary is separated into two distinct regions, the tropharium, housing the nurse cells, and the vitellarium, containing the developing oocytes (Figures 1 & 2) (Huebner, 1984). The nurse cells are connected to the developing oocytes via the trophic core and the trophic cords, to each individual oocyte. The oocytes lie in developmental succession, with only one vitellogenic oocyte per ovariole (Huebner, 1984). In addition to the dynamics of the oocyte cytoskeleton, the oocyte cortex in general undergoes changes during oogenesis.

The plasmalemma of previtellogenic oocytes (50 - 150uM in length) is smooth (Figures 3 & 4). The oolemma is closely apposed to the follicular epithelium (Figure 5). There is no evidence of pinocytosis at these early stages of previtellogenesis. The increase in oocyte size is due to the accumulation of materials transported down the trophic cords from the nurse cells (Huebner, 1984). Mitochondria, rough endoplasmic reticulum (RER) and numerous free ribosomes are

sparsely scattered throughout the cortex (Figure 5).

By mid-vitellogenesis oocytes are approximately 200-300uM in length. At this stage the follicular epithelium and the oolemma are still in close apposition (Figure 6 & 7). Various organelles have begun to accumulate in the cortical cytoplasm. Mitochondria are distributed deeper in the cortex, many of which appear to be dividing (Fig. 6). Golgi complexes are sparsely distributed in the cortex and the cisternae are flattened and small suggesting very little activity (see inset). Microvilli begin to form and the onset of pinocytotic activity is evidenced by the presence of patches of clathrin coated membrane and a few coated vesicles in the oocyte cortex (Figure 8).

Endoplasmic reticulum (ER) of two types is found in the ooplasm. The least apparent form of ER in the oocyte cortex is smooth ER (Figure 9). The rough ER (RER) is found in two forms in Rhodnius oocytes. Besides the conventional form of RER cisternae (Figure 10) there is a second distinctive form found in whorls with the cisternae closely linked together (Figure 11). This form of RER appears to be a novel form of packaging.

Just prior to vitellogenesis, follicles are 350-400uM in length, the oolemma becomes elaborated into prominant microvilli (Figure 12). Intercellular spaces between adjacent follicle cells and around the oocyte have not yet formed. A cortical cytoskeleton, which excludes large organelles, has developed (Figure 12). Mitochondria and annulate lamellae are found in the deeper cortex. Mitochondria are also scattered throughout the ooplasm.

RER in large whorls (Figures 13 & 14) is found in the deeper cortex of previtellogenic oocytes. In these whorls ribosomes are only found on the face of the cisterna that faces the cytoplasm. The cisternal faces which abut other cisterna are devoid of ribosomes. These layered cisternae appear to be linked by what appears to be a fibrous material when viewed in tangential section. Oblique section profiles of a portion of these ER whorls reveals spiral polyribosome units (Figure 13). Polyribosomes are not commonly found in the ooplasm. The developing oocyte does not synthesize proteins at a significant level (Huebner, 1984).

During vitellogenesis the follicle cells have separated forming large intercellular spaces. The

oocyte surface is covered with short finger-like microvilli. This is easily visualized by scanning electron microscopy of a denuded oocyte approximately 600uM in length (Figure 15). There is an anterior band of microvilli that is distinct (Figure 16) from the rest of the oocyte surfaces, particularly the lateral one. The anterior follicle cells of this area are also distinct from the lateral follicle cells. The micropyles in the chorion are formed by a distinct population of follicle cells in a narrow band between the cap and the lateral surface of the oocyte. During vitellogenesis most of the cytoplasm becomes restricted to the cortex as the yolk spheres accumulate (Figures 18 & 19). Partial Triton X-100 extraction of oocyte preparations for scanning electron microscopy removes some of the soluble cytoplasmic contents revealing yolk spheres (Figure 19).

At approximately 1400uM, prior to chorionation, numerous coated vesicles are still found in the cortex and microvilli still cover the surface (Figure 20). Annulate lamellae are occasionally found in the cortex (see inset) but they are more prevalent in the previtellogenic follicle. A geometrical pattern of microvilli has developed on the oocyte (Figure 21).

The microvilli that abut the apical follicle cell surface (adjacent to the oocyte) are short, whereas, those that extend towards the intercellular spaces in between the follicle cells are longer. In Figure 22 some of the follicle cells have been sheared away leaving only their bases. This illustrates the strong physical linkage between the follicle cells and the oocyte plasma membrane.

DYNAMICS OF THE MICROFILAMENT CYTOSKELETON

In order to determine the formation of an actin cytoskeleton various techniques were used to present an accurate analysis of the in vivo conditions. Rhodamine conjugated phalloidin, a stain specific for F-actin, and indirect immunofluorescence on diethylene glycol distearate (DGD) sections provide a good general overview of the magnitude and organization of the actin network which can then be augmented and extended with electron microscopy, both transmission and scanning. Scanning electron microscopy was carried out on detergent extracted and intact follicles. It was necessary to remove the follicle cells so that the oocyte surface could be examined.

Previtellogenesis

Oocytes smaller than 100-150uM in length do not exhibit a discernible actin cytoskeleton by any of the methods used (micrographs not shown). There is an intense rhodamine phalloidin staining in the tropharium that characterizes the F-actin meshwork that surrounds that microtubule packed trophic core and cords (Figure 23) (Gutzeit and Huebner, 1986). Oocytes 150-160uM in length, begin to reveal a faint rhodamine phalloidin staining in the cortex (Figure 23 & 24).

The cytoplasm of the unextracted previtellogenic oocyte is homogeneous with the cytoskeletal elements undiscernible (Figure 25). The entry of the trophic cord is evident by the presence of the microtubules in the anterior left of the oocyte. The surface is sparsely covered by microvilli (Figure 26).

Oocytes at mid to late stages of previtellogenesis, 250-350uM in length, have an increasing number of microvilli (Figure 27 & inset). Immunofluorescent staining of F-actin in DGD sections at this stage of oogenesis produces an intense band of fluorescence in the cortex (Figure 28). The microvilli have a microfilament core, which is evident by the

fluorescence staining pattern seen with rhodamine phalloidin (Figures 29 & 30). The surface view of the isolated cortex illustrates the abundance of microfilaments and the discrete pattern that has formed (Figure 30).

The underlying cortical cytoskeleton influences the contours of the oocyte plasma membrane (Figure 31 & 32). While the anterior oocyte surface where the trophic cord is attached is smooth there is an abrupt change from a smooth membrane to a microvillar rich surface (Figure 31) (see also Huebner, 1984). Immunofluorescent staining indicates that F-actin is present in the cortex underneath both the smooth and the microvillar membrane (Figure 32).

Transmission electron micrographs confirm the presence of microfilaments in the microvilli and in the cortex (Figure 33 & 34). The microfilament core extends deep into the cortex of the oocyte.

In the later stages of previtellogenesis, there is an increasing number of microvilli covering the oocyte surface (Figures 35, 37 and 38). Elements of the cortical cytoskeleton are visible in extracted cleaved scanning electron microscopy preparations (Figure 37). While scanning electron microscopy allows one to detect

cytoskeletal elements in the cortex, it does not permit specific identification of type. Immunofluorescence staining of the lateral region of the oocyte results in a brilliantly fluorescent cortex (Figure 38). This band illustrates the significant amount of actin present in the oocyte cortex. This actin is not all in the form of F- actin as is evident with the phalloidin stain. The type of buffer as well as the time in buffer is an important parameter in the examination of the cortex. When denuded oocytes are kept in saline for extended periods of time, elongated microvilli form (Figures 39, 40 & 41) (see also Huebner, 1984). Presumably this results in conditions allowing the polymerization of G- actin. This oocyte (Figure 39) has been extracted in Triton X-100 for a short time and the elongated microvilli have been sheared away so that the underlying cortex is visible (Figure 39 & 41). In the underlying cortex one cannot identify individual cytoskeletal elements as they appear to be so tightly woven (Figure 41). The individual elongated microvilli are found clumped together (Figure 40). These results also show that the actin mesh of the cortex consists of a superstructure of microvillar core actin and an underlying mat of filaments and that these can be

separated by shearing.

Vitellogenesis

Throughout vitellogenesis the lateral follicle cells remain separated and yolk spheres accumulate in the oocyte cytoplasm (Figure 42). The prominant cortical actin band seen with immunofluorescence staining (Figure 42) is confirmed by transmission electron microscopy (Figure 43). Microfilaments form the microvillar core and form a network underneath the plasma membrane.

In an unextracted cleaved oocyte the cortex is visible but one cannot distinguish any filaments from the soluble proteins (Figure 44). Extracted preparations of lateral follicle cells and the isolated oocyte cortex facilitate the visualization of cytoskeletal elements (Figure 45). The follicle cell microvilli indent deeply into the oocyte cortex (Figures 36, 45 & 46). These extensions of the follicle cells have a microfilament core. Thus, when examining preparations with the follicle cells left on the surface, one has to have caution in attributing staining totally to the oocyte.

During vitellogenesis the follicle cells have separated creating large spaces between adjacent follicle cells and around the oocyte. Scanning electron microscopy and rhodamine phalloidin staining of whole mount preparations illustrate the effect that the follicular epithelium has on the contour of the oolemma (Figures 47, 48, 49, 50 & 51). The distinct pattern of microvillar formation on the oocyte with microvilli lying underneath the follicle cells being shorter than those extending into the intercellular spaces becoming longer. Rhodamine phalloidin staining indicates that these microvilli have microfilament cores (Figures 47, 48, 50 & 51). The lateral follicle cells have been removed so that this staining is completely attributable to the microfilaments in the oocyte cortex. Rhodamine phalloidin staining of isolated cortices complements the analysis of whole mounts illustrating that the same pattern of microvilli is revealed by different techniques. Transmission electron microscopy confirms that the staining coincides with the distribution of microfilaments in the oocyte cortex (Figures 52 & 53).

During vitellogenesis the anterior follicle cells do not separate as do the lateral follicle cells

(Figure 54). There is a distinct boundary between the anterior and the lateral regions. The fluorescence pattern of actin staining indicates that there is a difference in the oocyte cytoskeleton from the anterior to the posterior regions. The intense staining pattern that is found in the lateral oocyte cortex (Figures 54 & 55) is absent from the anterior cortex (Figure 54). The microfilament rich oocyte cortex ends abruptly in the transition zone between the lateral and apical follicle cells (Figure 54).

Once the follicle reaches 1400uM in length, vitellogenesis is almost complete (Figure 56). Spaces between the follicle cells and oocyte are still present as are numerous coated vesicles in the cortex. Figure 57 displays the abundance of microfilaments still found in the cortex. Many organelles are excluded because of the tightly woven network of cytoskeletal elements.

DYNAMICS OF THE MICROTUBULE CYTOSKELETON

Previtellogenesis

The dynamics of the microtubule cytoskeleton differs significantly from those of the microfilaments. The smaller oocytes, 50-150uM in length, do not appear to have a discernible microtubule cytoskeleton, although there is a punctate fluorescence pattern throughout the cytoplasm (Figure 58, 59 & 60). This is probably due to pools of tubulin dimmers. The prominant trophic cord microtubules into the oocyte are visualized by sectioned material (Figures 59 & 60) and by scanning electron microscopy (Figures 25 & 31) verifying that other areas of the same preparation reveal microtubules. The trophic cord microtubules extend deeply into the oocyte cortex, fanning out and dispersing into fine wavy strands as the oocyte enlarges. By mid-previtellogenesis, approximately 250uM, tubulin staining is prominent throughout the entire oocyte cytoplasm revealing an abundance of microtubules (Figure 61). Because one is visualizing a much thinner section, transmission electron microscopy

microtubules (Figure 63). Micrographs confirm the presence of microtubules and show that they often are parallel to the oolemma (Figure 63). This also stresses the need for complementary techniques and that immunofluorescence provides for an overview assessment of the magnitude of the microtubule complement.

The lateral regions of the late previtellogenic oocyte have a well defined cortical microtubule cytoskeleton (Figure 62). The presence of microtubules is confirmed by transmission electron microscopy (Figure 63 & 65). The abundance of tubulin in the oocyte cortex is well visualized by immunofluorescence staining of DGD sections through the oocyte cortex (Figure 64).

Vitellogenesis

During early vitellogenesis the oocytes range from 350-450uM in length. The lateral follicle cells have begun to separate, while the anterior and the posterior follicle cells remain closely apposed to one another and to the oolemma. Unlike the actin distribution, the anterior oocyte cortex appears to have a well defined microtubule cytoskeleton. This is probably due, at

least in part to the extension of trophic cord microtubules (Figure 67). They enter the oocyte cortex and splay out. The posterior region of oocytes at this stage of early vitellogenesis also has a distinct cortical microtubule cytoskeleton (Figure 68). This is evident by the brilliant band of fluorescence seen with Anti-tubulin staining. The lateral regions differ from the anterior and the posterior cortex as seen with immunofluorescence staining (Figure 70). There is a distinct boundary between the anterior and the lateral cortex. The amount of cortical microtubules in the anterior region of the oocyte diminishes so that in the lateral cortex there are comparably fewer microtubules (Figure 70).

The lateral microtubule pattern remains sparse throughout vitellogenesis (Figures 72, 74, 75 & 76). The oocyte continues to take up yolk proteins from the hemolymph filling the cytoplasm with yolk spheres (Figures 71 & 73).

Controls

The indirect immunofluorescence methods for DGD sectioned materials have been developed for Rhodnius

prolixus ovarioles by Gunnar Valdimarsson. I have only modified the incubation times slightly. Controls omitting the primary antibody, for both Anti-actin and Anti-tubulin, were performed resulting in no background fluorescent pattern. The presence of known microtubules in the trophic core and cords provides for in situ controls for the tubulin preparations (Figures 58, 59, 60 & 67). The use of the specific binding of Rhodamine-phalloidin and Anti-actin provides two independent methods for examining the actin patterns. The correlation between the results obtained with these two methods increases the level of confidence that the results obtained truly reflect the topographical and organizational changes in actin abundance that are seen during oogenesis.

BIOCHEMISTRY

A Western Blot of an SDS polyacrylamide gel of an ovary homogenate was prepared in order to confirm the actin staining specificity of the antibody used for DGD staining. The Silver stained gel is a replicate of the gel that was used for the Western Blot (Figures 77 & 78). The gel was overloaded in order to visualize the

colour reaction on the blot. A purified actin preparation was also run as a control. It ran at the expected molecular weight of 42Kd. However, unexpectedly, both the ovary sample and the embryo (results of G.M. Kelly) samples stained for actin at approximately 63Kd. While the discovery of this actin in the ovary is significant it is beyond the scope of this thesis. Further analysis of this unusual actin form is under investigation by G.M. Kelly and P.S. McPherson using primarily Rhodnius prolixus embryos.

ABBREVIATIONS

AL = Annulate Lamellae

FC = Follicle Cell

G = Glycogen

GV = Germinal Vesicle

MF = Microfilament

MV = Microvilli

N = Nurse

O = Oocyte

SEM = Scanning Electron Microscopy

TEM = Transmission Electron Microscopy

TC = Trophic Cord

Y = Yolk

PLATE 1

General Features of the Oocyte Cortex
Previtellogenesis

Figures 1-3 — Brightfield micrographs illustrating the structure of the telotrophic ovariole. Note the trophic cords leading to the oocytes (asterisk, TC). The follicular epithelium and the oolemma are closely apposed (arrowheads). X150, X575, X500

Figure 4 — SEM micrograph of a denuded oocyte approximately 40uM in length. Note the smooth surface. X1,900

Figure 5 — TEM micrograph of oocyte cortex. Note the smooth oocyte membrane and adjacent follicle cells (arrows). X68,000

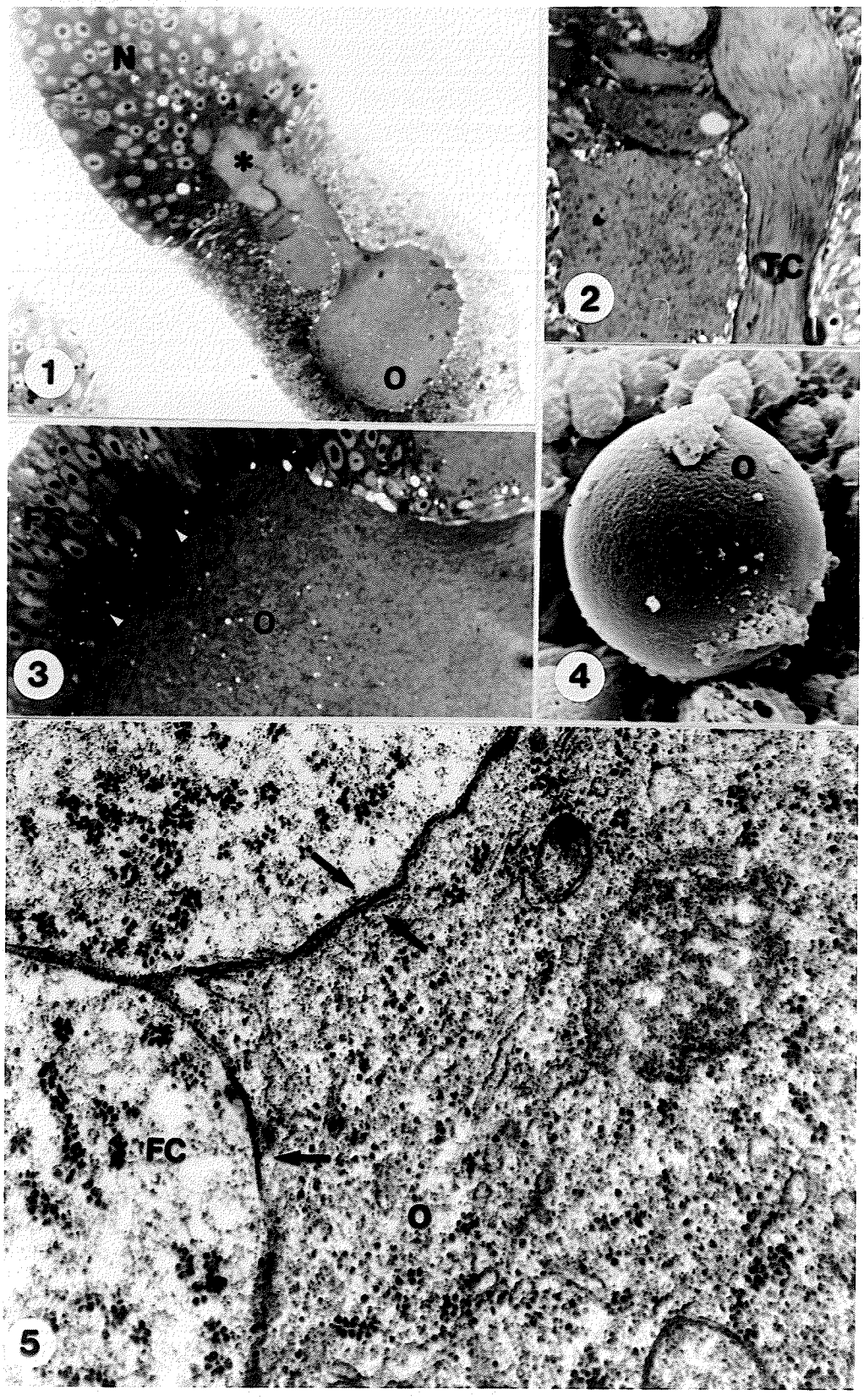
N
*
O
1
TC
2
O
3
4
FC
O
5

PLATE 2

General Features of the Oocyte Cortex
Mid-Previtellogenesis

Figure 6 — TEM micrograph of oocyte, 200-300uM in length, cortex. Microtubules run parallel to the oocyte surface (arrowheads). Mitochondria and Golgi complexes are found in the cortex (insets). X31,350, X24,350, X19,800

Figure 7 — Brightfield micrograph illustrating the apposition of the follicular epithelium and the oolemma (arrowheads). X640

Figure 8 — TEM micrograph of mid-previtellogenic oocyte cortex. Note the appearance of microvilli projecting into the follicle cell (asterisk)and the evidence of pinocytotic activity (arrows). X49,000

Figures 9 10 & 11 — TEM micrographs illustrating the configurations of endoplasmic reticulum (ER) (arrows) in the oocyte. Fig. 9 is smooth ER, Fig. 10 is the conventional form of rough ER, and Fig. 11 is a novel form of rough ER packaging. X48,000, X37,500, X37,500

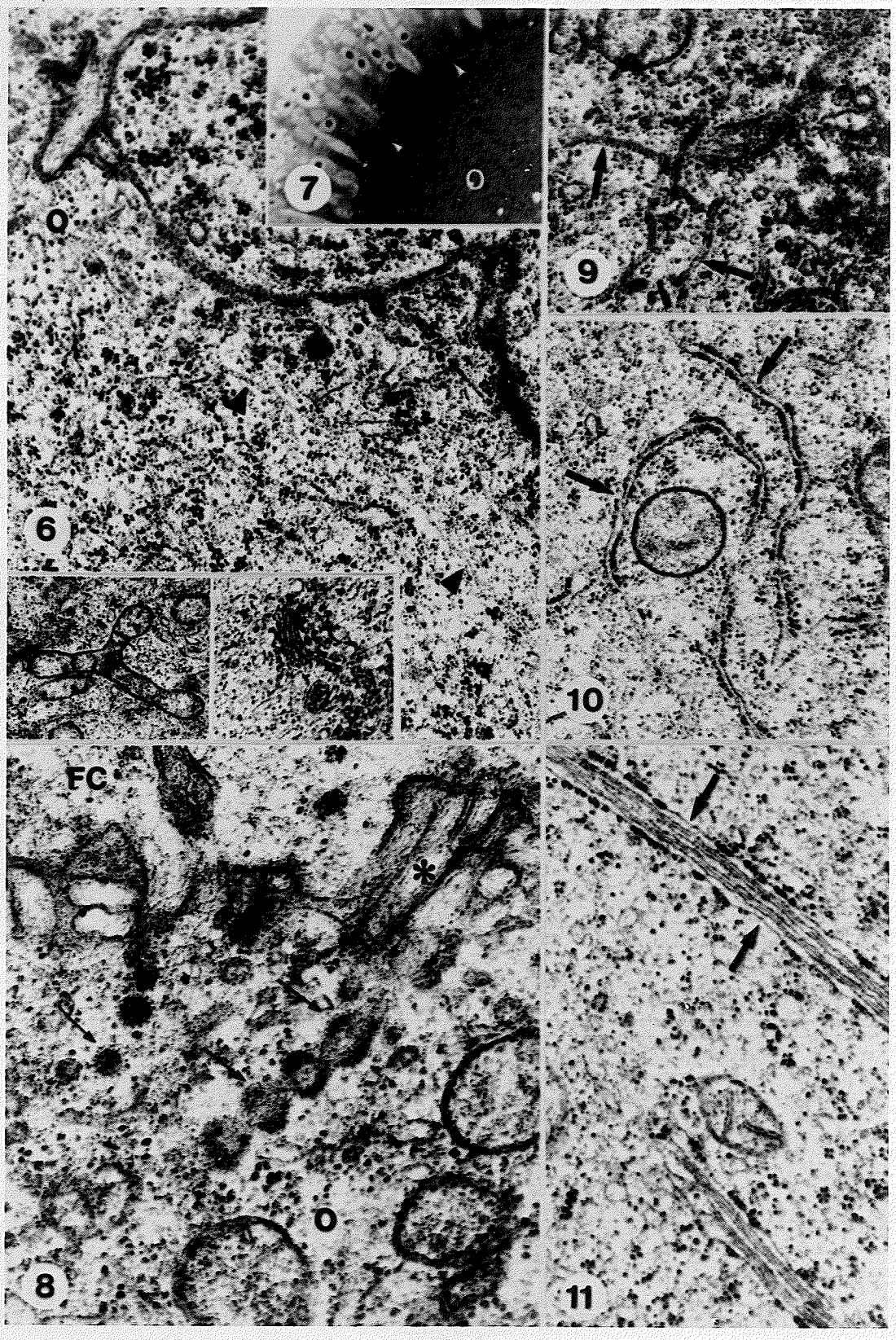
Q
7
Q
9
6
10
FC
*
Q
8
11

PLATE 3

General Features of the Oocyte Cortex
Late Previtellogenesis

Figure 12 — TEM micrograph of the oocyte cortex, approx. 300-400uM in length. Note the abundance of microvilli (MV) and annulate lamellae (AL) in a deeper region the cortex. X12,000

Figure 13 — TEM micrograph of the novel configuration of rough ER in the ooplasm. The cisternae are arranged in closely linked (arrows and asterisk) whorls. Ribosomes are found in groups on the outer cisterna (arrowheads). X48,000

Figure 14 — TEM micrograph of rough ER illustrating the presence of spiral polyribosomes and the ER cisternae (arrows). X24,000

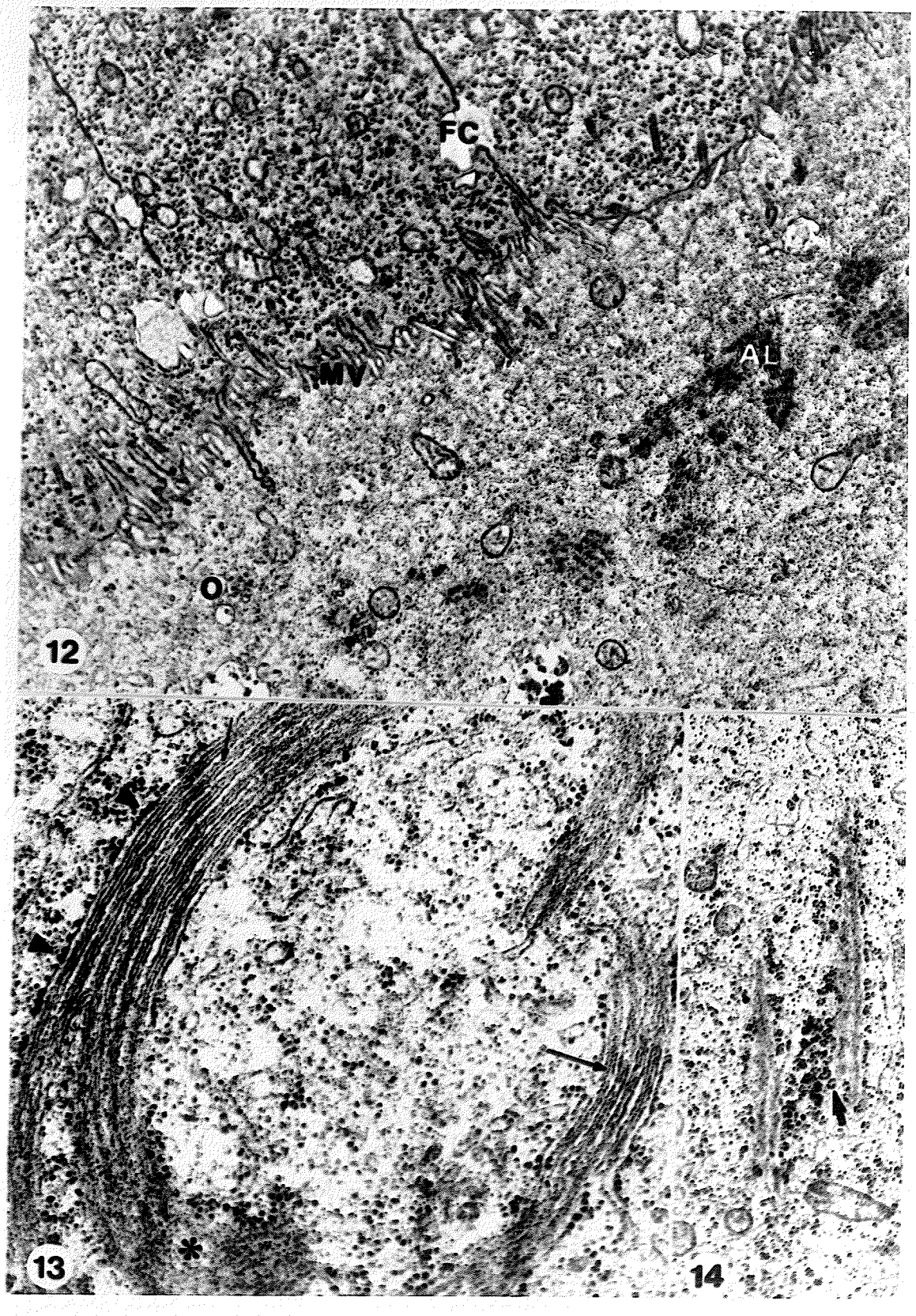
FC
MV
AL
O
12
13
14

PLATE 4

General Features of the Oocyte Cortex
Mid-vitellogenesis

Figures 15 & 17	SEM micrograph of denuded vitellogenic follicle highlighting regional differences in the contours of the oolemma. Note the distinct band of microvilli (arrows) in the anterior region. Fig. 17 is high magnification of this area. X240, X1,500
Figure 16	SEM micrograph of intact vitellogenic follicle (asterisk denotes the anterior region of oocyte). X50
Figures 18 & 19	SEM micrograph illustrating the intercellular spaces between the follicle cells (arrow) and the abundance of yolk spheres (Y). Note, the exposed oolemma is covered with microvilli (asterisk). X900X, X500

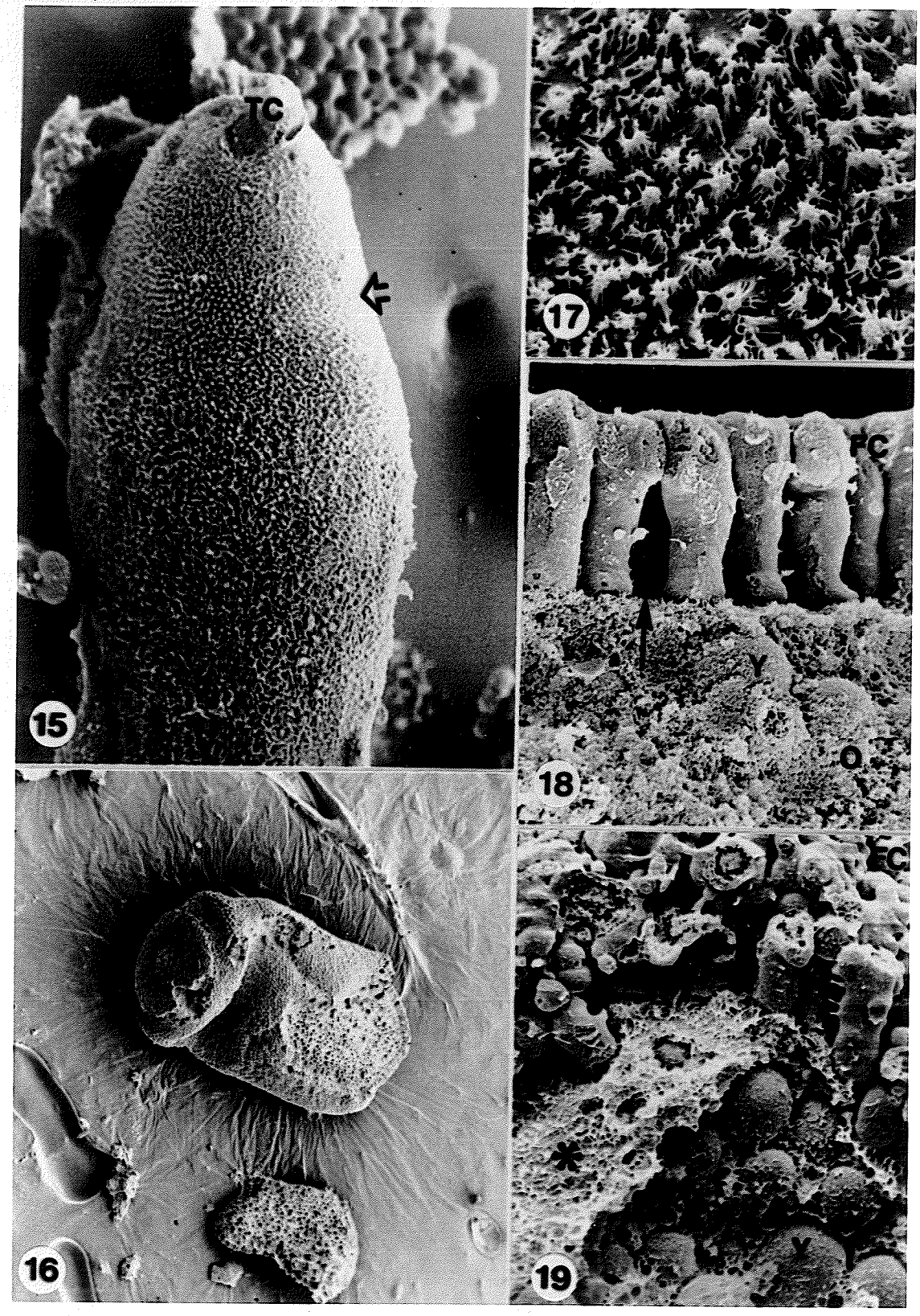
TC
15
17
FC
Y
O
18
FC
Y
19
16

PLATE 5

General Features of the Oocyte Cortex
Late-Vitellogenesis

Figure 20 — TEM micrograph of late vitellogenic follicle. Note the presence of clathrin coated vesicles (arrows) and microfilaments forming the microvillar core and in the underlying cortex (arrowheads). Annulate lamellae (see inset) are sparsely distributed throughout the cortex. X71,000, X32,000

Figure 21 — SEM micrograph of late vitellogenic follicle. Note spaces between follicle cells and the processes that connect them (arrowheads) and the microvilli covering the oocyte surface (arrow). X3,000

Figure 22 — SEM micrograph of lateral region of follicle in which the follicle cells have been sheared away leaving their bases attached to the oolemma (arrow). X950

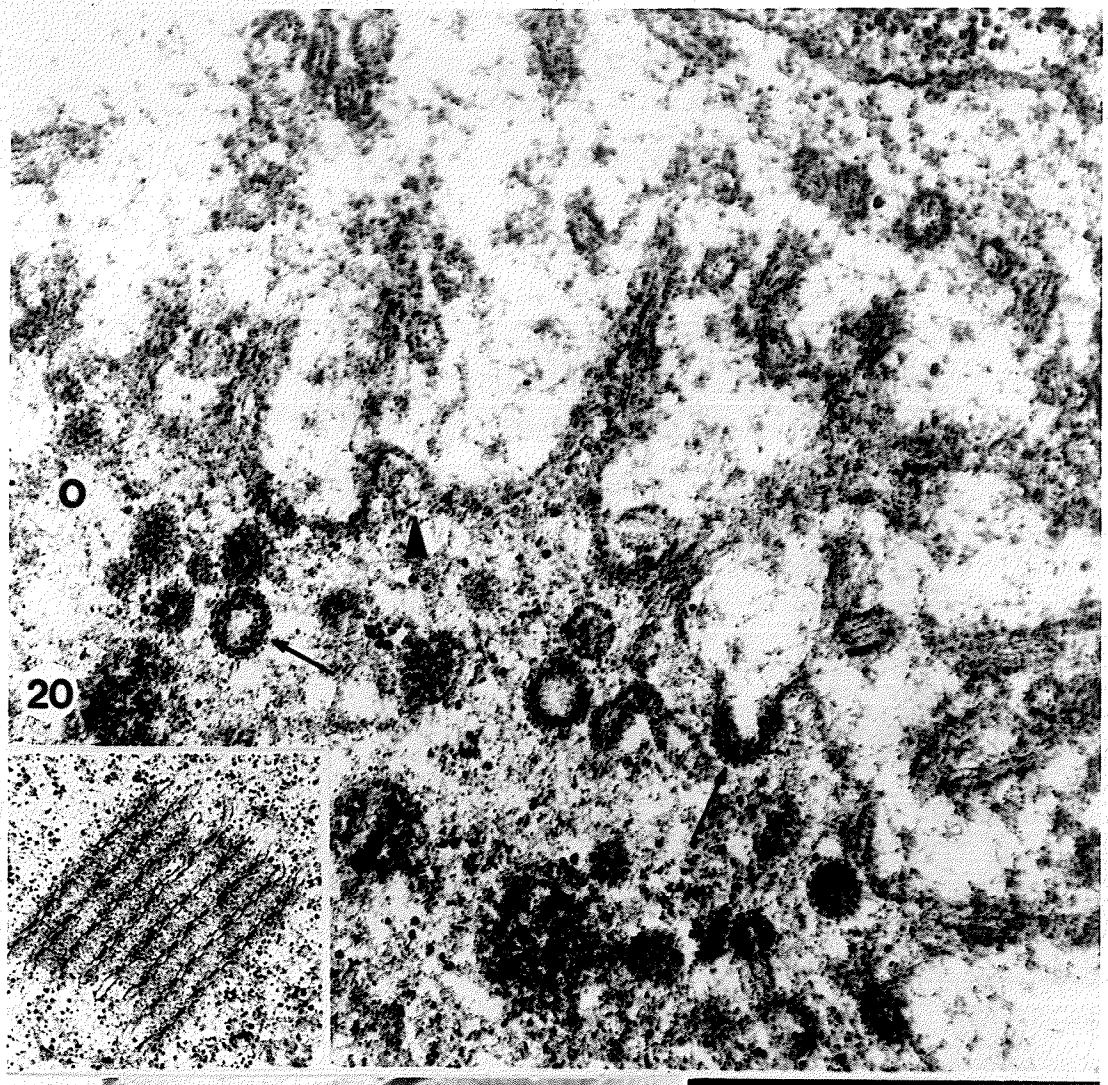
O
20

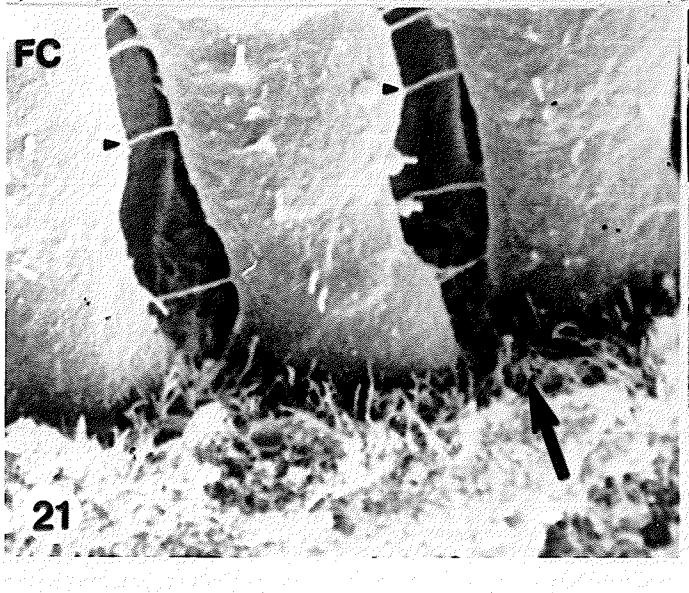
FC
21

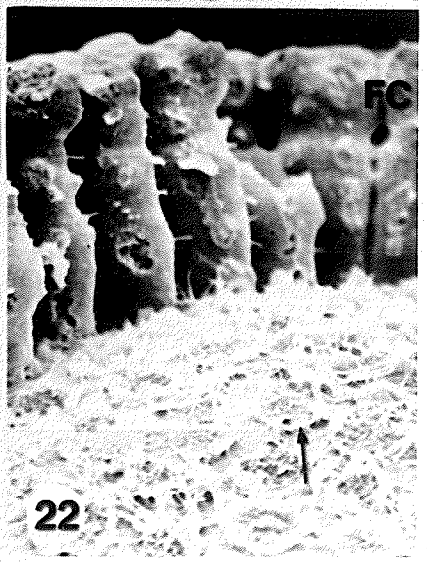
FC
22

PLATE 6

Dynamics of the Microfilament Cytoskeleton
Previtellogenesis

Figures 23 & 24 — Rhodamine phalloidin staining of denuded whole mounts. Note the intense fluorescence of the trophic core meshwork (asterisk) and the bands of F-actin in the trophic cords (arrows). The oocyte, 160uM, cortex stains faintly (arrowheads). X450, X650

Figures 25 & 26 — SEM micrograph of denuded unextracted oocyte, 160uM in length. The oocyte has been cleaved to view the cytoplasm. Note the extension of the trophic cord microtubules into the oocyte (arrow, Fig. 25). Note the small microvilli on the oocyte surface (arrows, Fig. 26). X750, X1,650

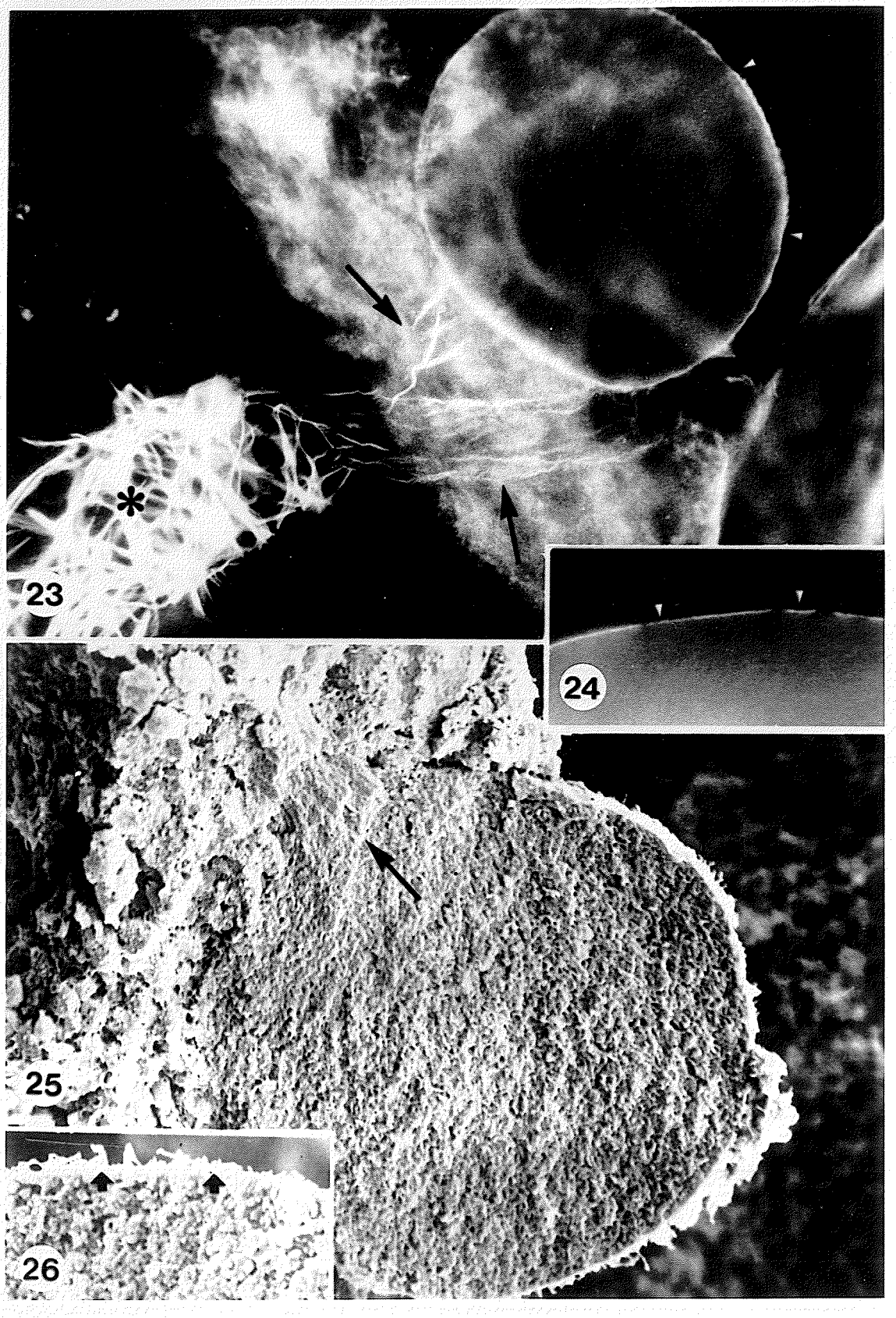
23
24
25
26

PLATE 7

Dynamics of the Microfilament Cytoskeleton
Mid-Previtellogenesis

Figure 27	SEM micrograph of a denuded oocyte, 250-300uM in length. Note the numerous microvilli covering the surface (see inset). X250, X1,500
Figure 28	Immunofluorescence micrograph stained for actin. Note the brilliant band of fluorescence in the cortex (arrowheads). X900
Figures 29 & 30	Rhodamine phalloidin stained whole mounts illustrating the significant amount of F-actin in the cortex (arrowheads) and the discrete pattern that is forming. X800, X800
Figure 31	SEM micrograph of the anterior region of the oocyte showing the entry of the trophic cord and the abrupt change in membrane topography that occurs (arrowheads). X1,300
Figure 32	Immunofluorescent micrograph illustrating the pattern of actin distribution (arrowhead) in the anterior cortex where the trophic cord enters. X1,000
Figures 33 & 34	TEM micrographs of oocyte cortex confirming the presence of mircofilaments in the microvilli and in the underlying cortex substructure (arrows). Note the extension of the microfilaments deep into the cortex (arrows, Fig. 33). X22,500, X44,000

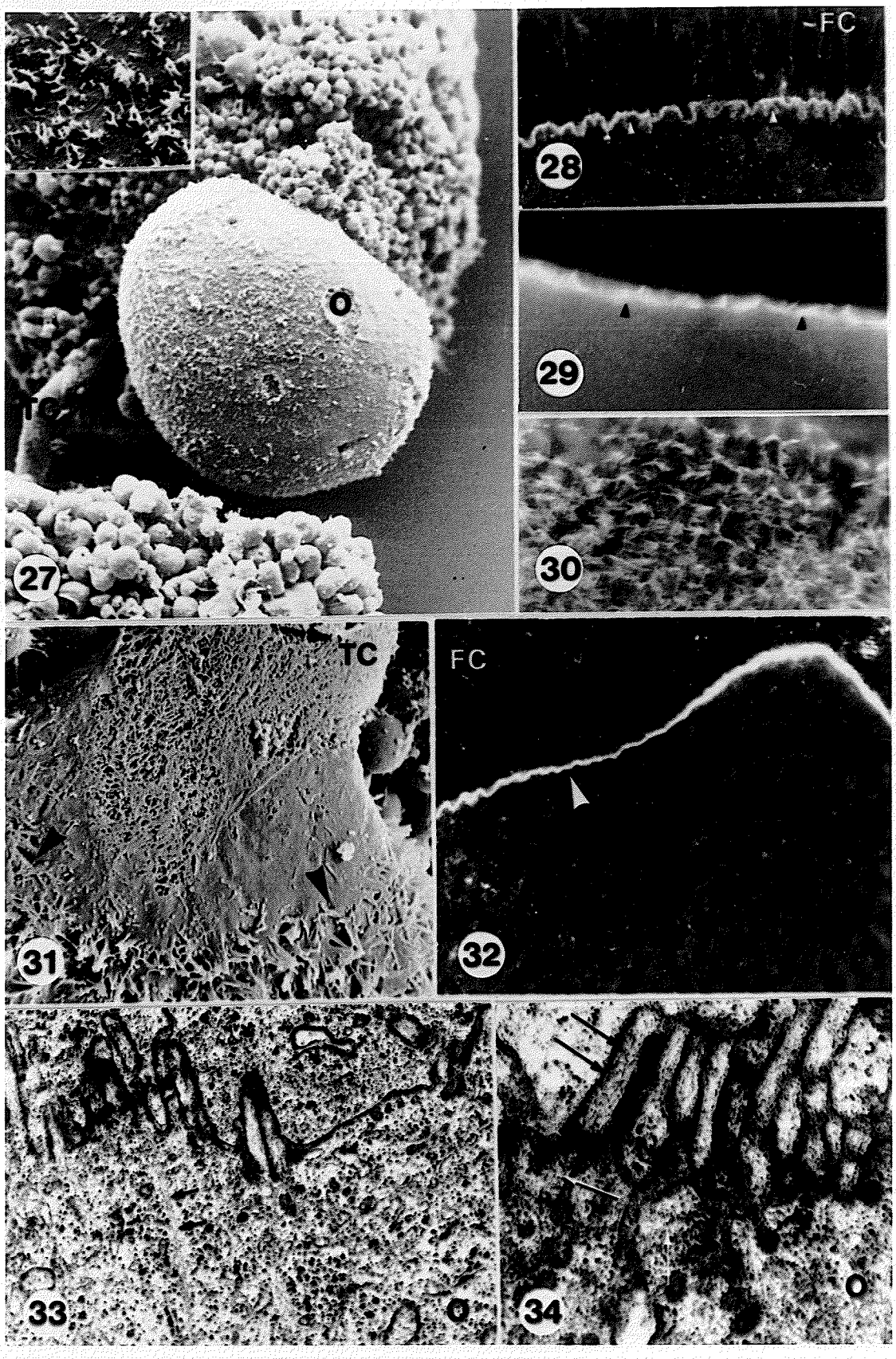
O
TC
27
FC
28
29
30
TC
31
FC
32
33
O
34
O

PLATE 8

Dynamics of the Microfilament Cytoskeleton
Late Previtellogenesis

Figure 35	TEM micrograph of oocyte cortex noting the abundance of microvilli (arrows) and the presence of a large whorl of rough endoplasmic reticulum (asterisk in Fig. 35). X16,600
Figure 36	TEM micrograph noting the microfilament containing microvillus of the follicle cell extending into the oocyte cortex. X78,000
Figure 37	SEM micrograph of partially extracted cleaved oocyte illustrating the presence of cytoskeletal elements in the oocyte cortex (arrowheads). X4,300
Figure 38	DGD section stained for actin. Note the brilliant band of fluorescence in the cortex (arrowheads). X1,250
Figures 39, 40 & 41	SEM micrograph of partially extracted oocytes illustrating the large amount of actin composing two layers of the cortex, microvillar microfilaments and underlying substructure of a tightly woven cytoskeletal network (asterisk). X900, X1,800, X1,600

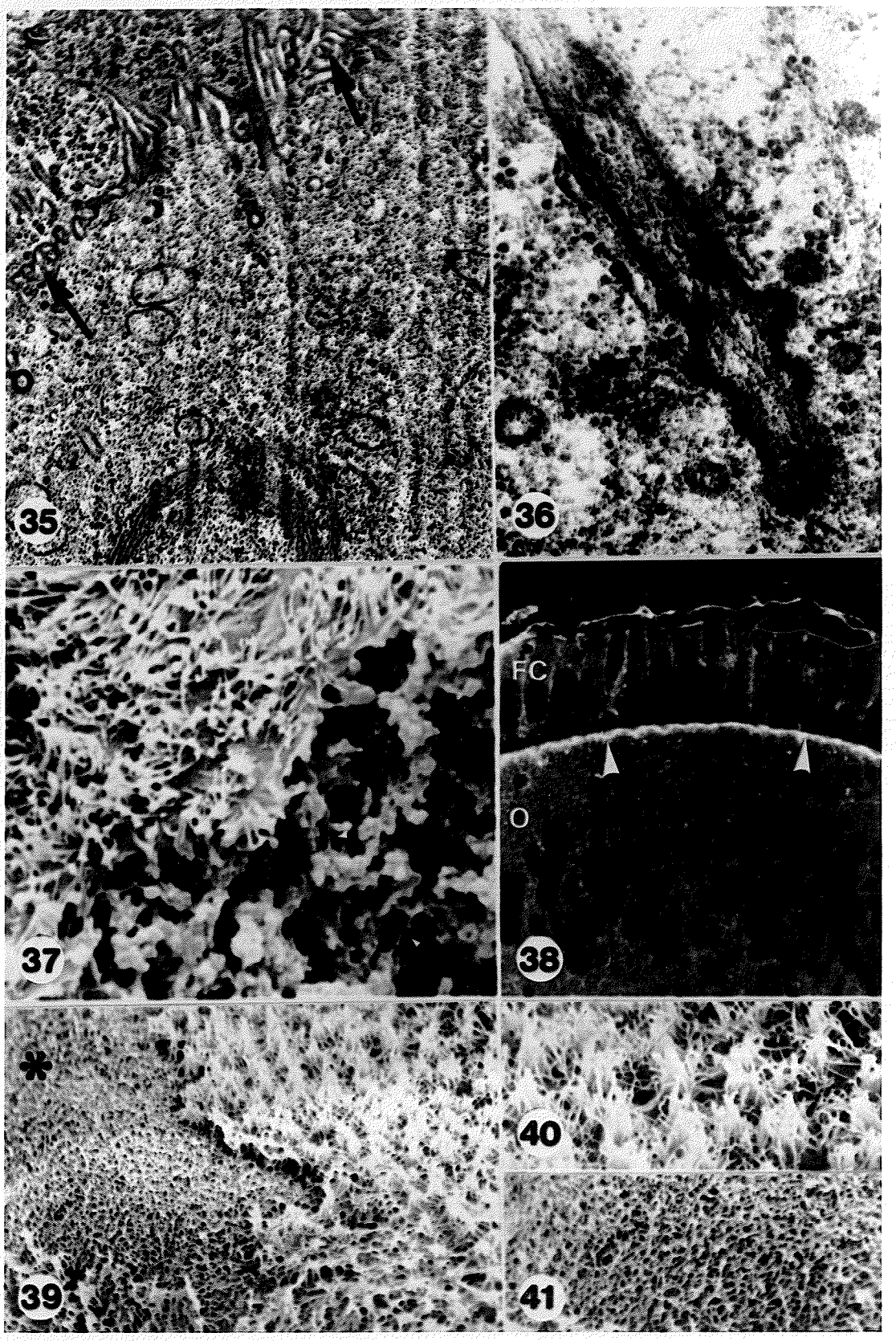
35
36
37
FC
O
38
39
40
41

PLATE 9

Dynamics of the Microfilament Cytoskeleton
Vitellogenesis

Figure 42 — Immunofluorescent micrograph illustrating the actin fluorescence in the cortex (arrowheads) and the spaces between the follicle cells. X650

Figure 43 — TEM micrograph confirming the presence of microfilaments in the oocyte microvilli (arrowheads). Note the presence of glycogen, G, and the lack of large organelles in the cortex (asterisk). X34,100

Figure 44 — SEM micrograph of cleaved non-extracted follicle. Note the homogeneous appearance of the cortex (asterisk) and the inability to discern details of the follicle cell and oocyte membranes (arrows). X1,700

Figure 45 — SEM micrograph of extracted isolated oocyte cortex and follicular epithelium showing the extensions of the follicle cells into the oocyte cortex (arrows) and the presence of cytoskeletal elements in the oocyte cortex (arrowheads). X1,700

Figure 46 — TEM micrograph illustrating the presence of microfilaments in the follicle cell extensions which protrude into the oocyte cortex (arrows). X62,000

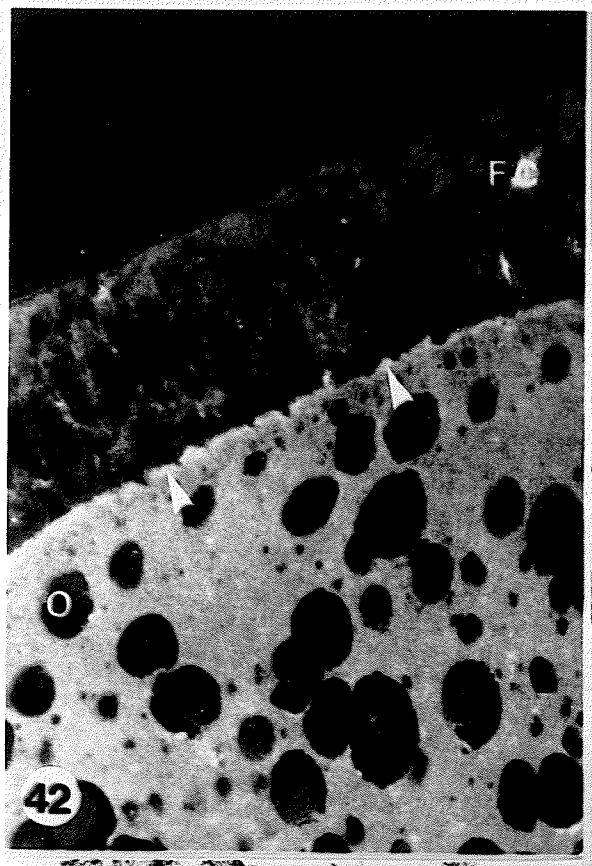
F
O
42

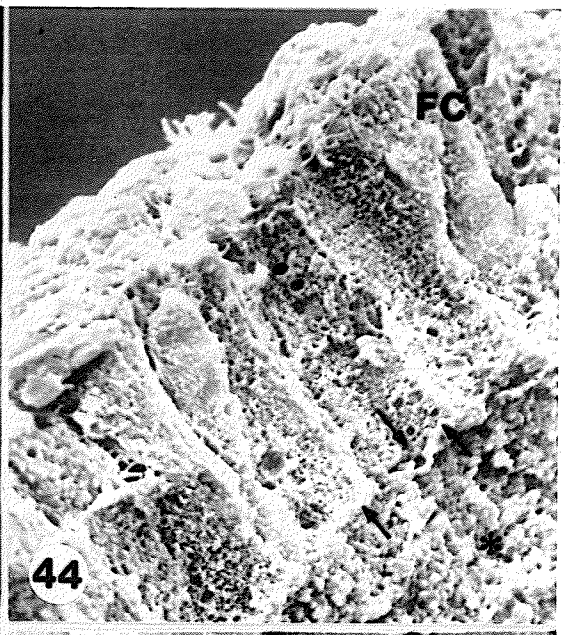
FC
44

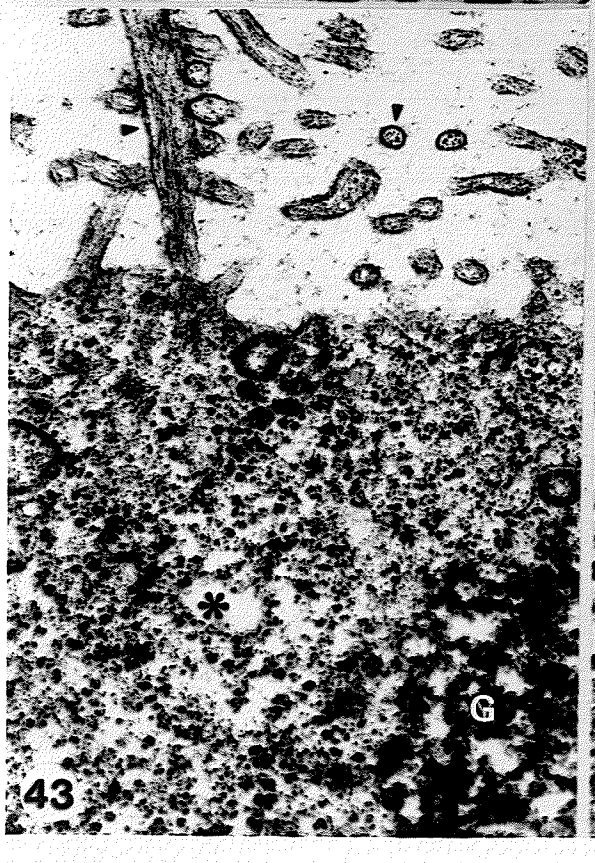
G
43

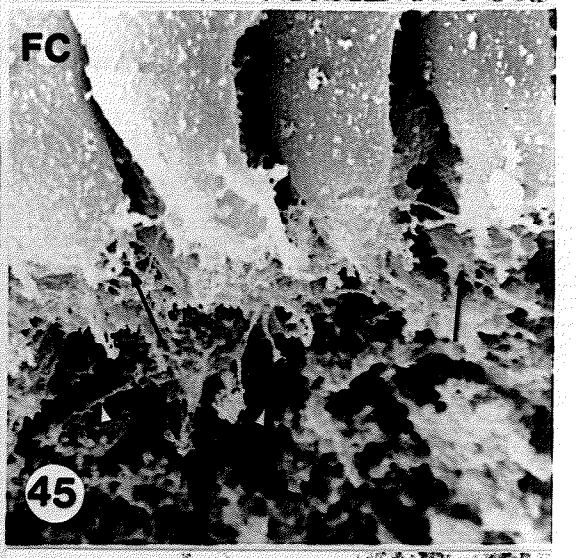
FC
45


46

PLATE 10

Dynamics of the Microfilament Cytoskeleton
Mid-Vitellogenesis

Figures 47 48 & 49	Rhodamine phalloidin staining and SEM of denuded oocytes illustrate the discrete microfilament pattern that has formed (asterisk denotes area where follicle cell would sit). X750, X900, X1,100
Figures 50 & 51	Rhodamine phalloidin staining of isolated cortices, thus attributing F-actin staining to the cortex and emphasizing the pattern of microfilaments (arrowheads). X400, X450
Figures 52 & 53	TEM micrograph confirms the presence of microfilaments in the microvilli (arrowhead) and in the underlying substructure. Note the presence of clathrin coated vesicles in the cortex (arrow). X40,900, X57,300

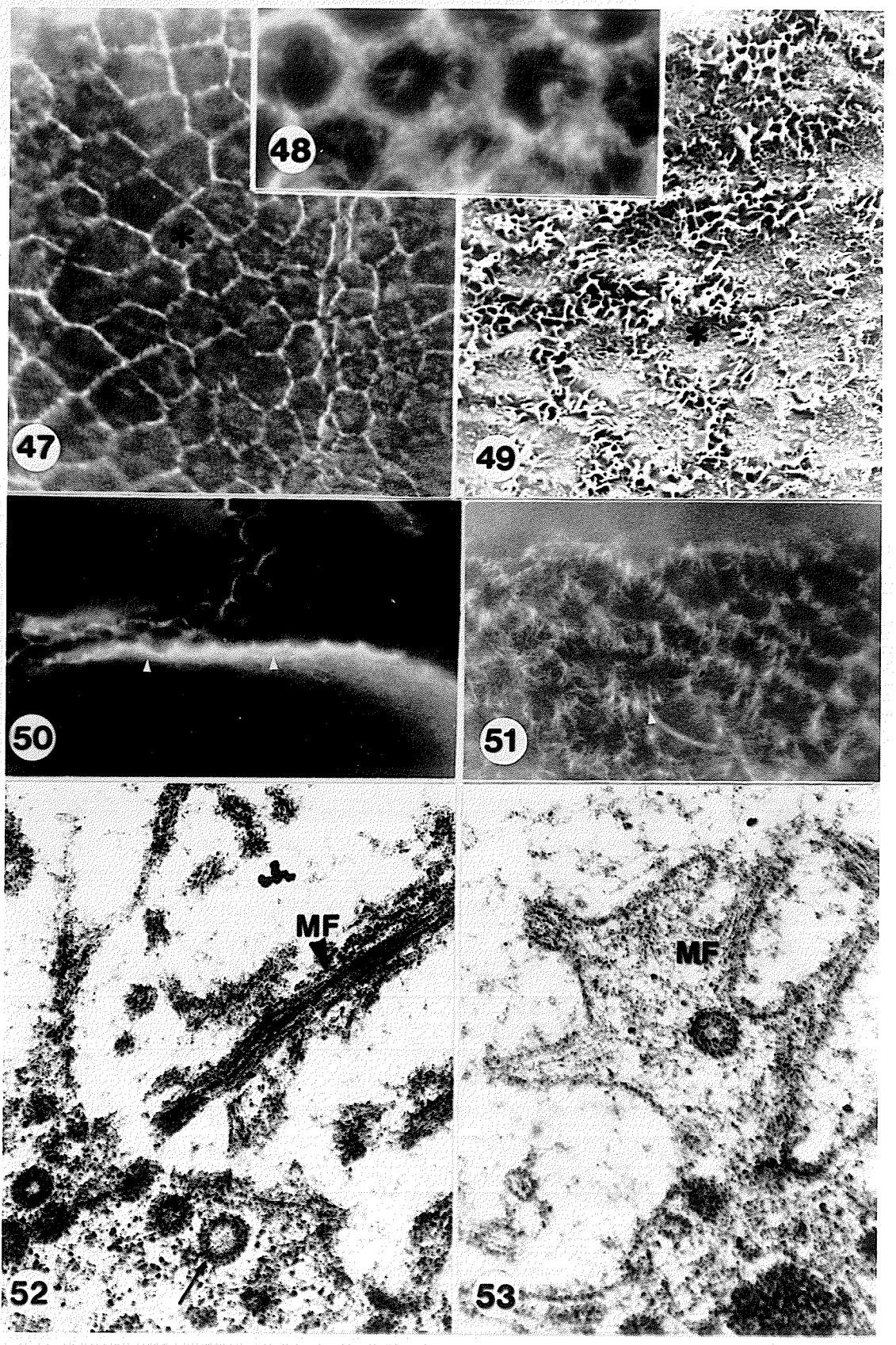
47
48
49
50
51
MF
52
MF
53

PLATE 11

Dynamics of the Microfilament Cytoskeleton
Late Vitellogenesis

Figures 54 & 55	Immunofluorescence sections of the anterior (Fig. 54) and lateral regions of the oocyte (Figs. 54 & 55) of a large follicle, approx. 1,200uM length. In Fig. 54 note the abrupt change in actin staining at the transition from lateral to anterior region (arrow). The asterisk denotes the lateral follicle cells). Note the brilliant band of fluorescence in the lateral cortex (arrowheads, Fig. 55). X1,300, X650
Figures 56 & 57	TEM micrograph denoting intercellular spaces and the abundance of microvilli (arrowheads, Fig. 56) and microfilaments (arrowheads, Fig. 57). Note the microtubule running parallel to the oocyte cortex (arrow, Fig. 57). X7,450, X35,000

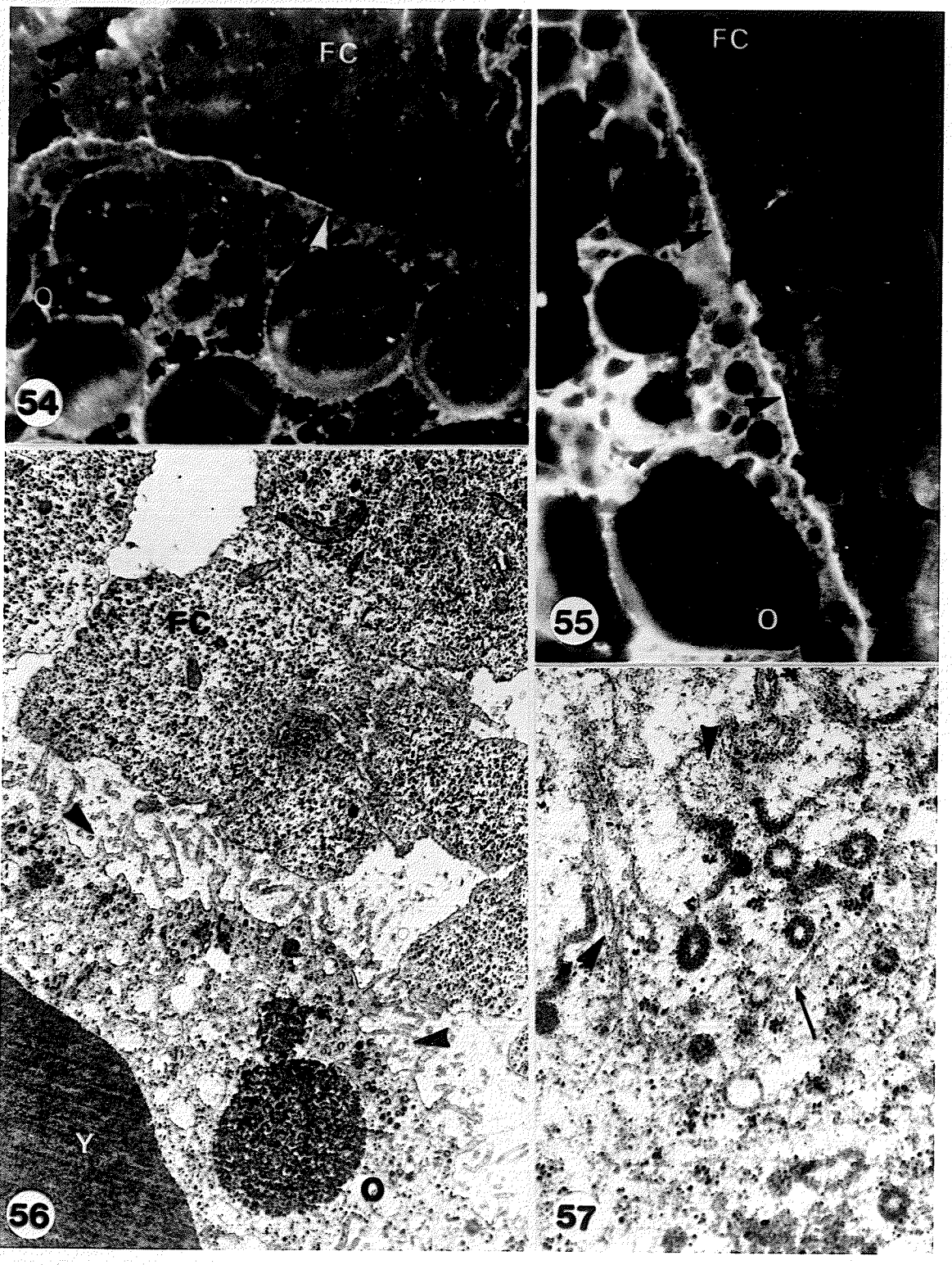
FC
O
54
FC
55
O
FC
Y
O
56
57

PLATE 12

Dynamics of the Microtubule Cytoskeleton
Previtellogenesis

Figures 58 - 61

DGD sections stained for tubulin. Note the brilliant fluorescence of the trophic cords invFigs. 58, 59 & 60. Note the central position of the germinal vesicle (GV) and the general staining pattern of the strands throughout the ooplasm of the small previtellogenic oocytes (asterisk). Figs. 59 & 60 illustrate the extension of trophic cord microtubules into the oocyte, splaying out into fine wavy strands (arrowheads). Fig. 61 is an oocyte, approx. 300uM in length, that has developed a defined microtubule cortex (arrows). X550, X750, X550, X1,300

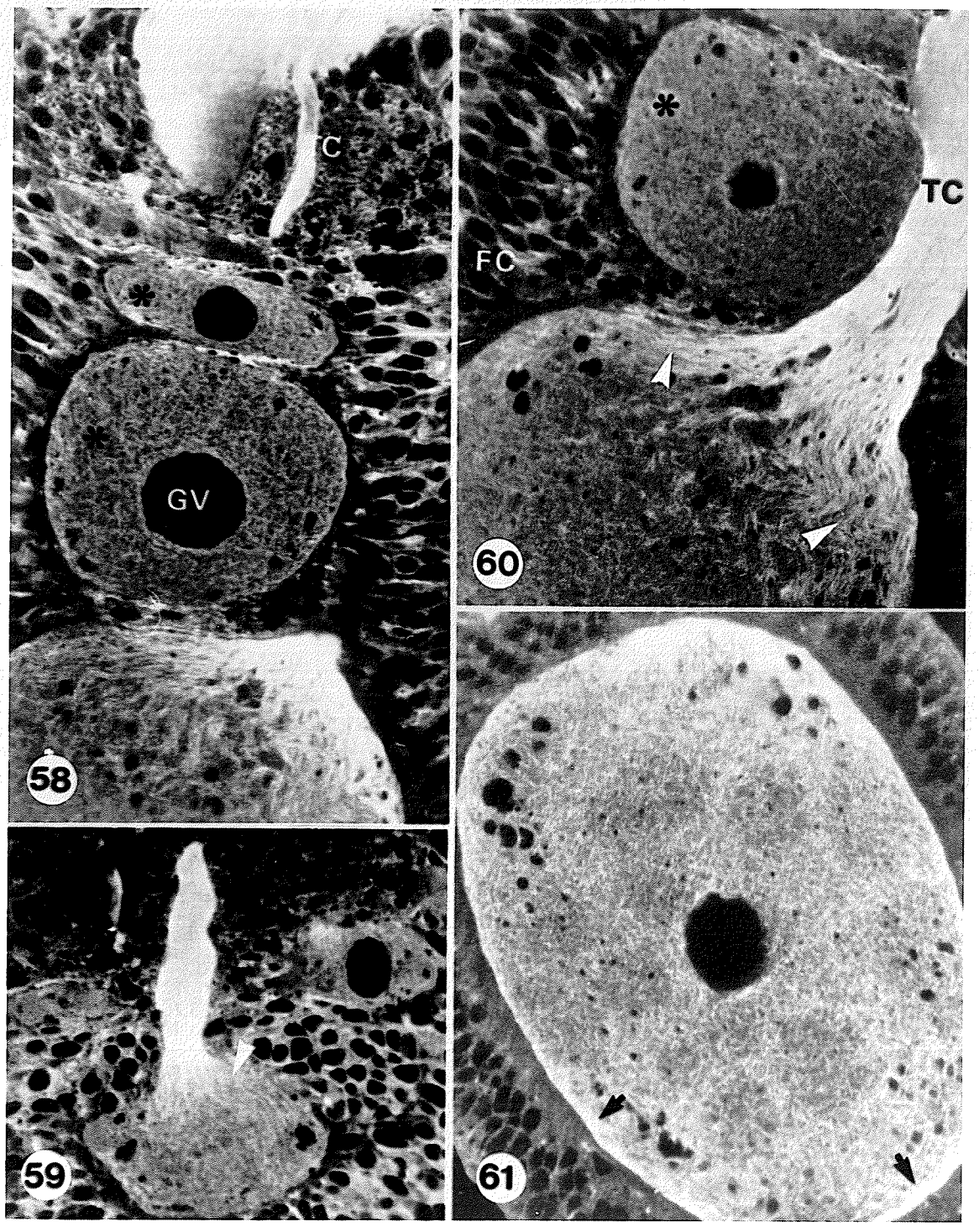
C
GV
58
TC
FC
60
59
61

PLATE 13

Dynamics of the Microtubule Cytoskeleton
Late Preitellogenesis

Figure 62 — Immunofluorescence micrograph showing the intense tubulin staining pattern in the cortex (arrowheads). Note the general distribution of strands throughout the rest of the ooplasm. X2,150

Figure 63 — TEM micrograph confirming the presence of microtubules in the cortex, illustrating their orientation parallel to the oolemma (arrowheads). X48,400

Figure 64 — Immunofluorescence micrograph through the cortex indicating the overwhelming amount of microtubules. Note the wavy strands of trophic cord microtubules in the anterior region of the oocyte (asterisk). X1,950

Figure 65 — Higher magnification TEM micrograph of microtubules in the cortex (arrowhead). X75,000

Figure 66 — Brightfield micrograph illustrating overall structure of the follicle at this stage. X650

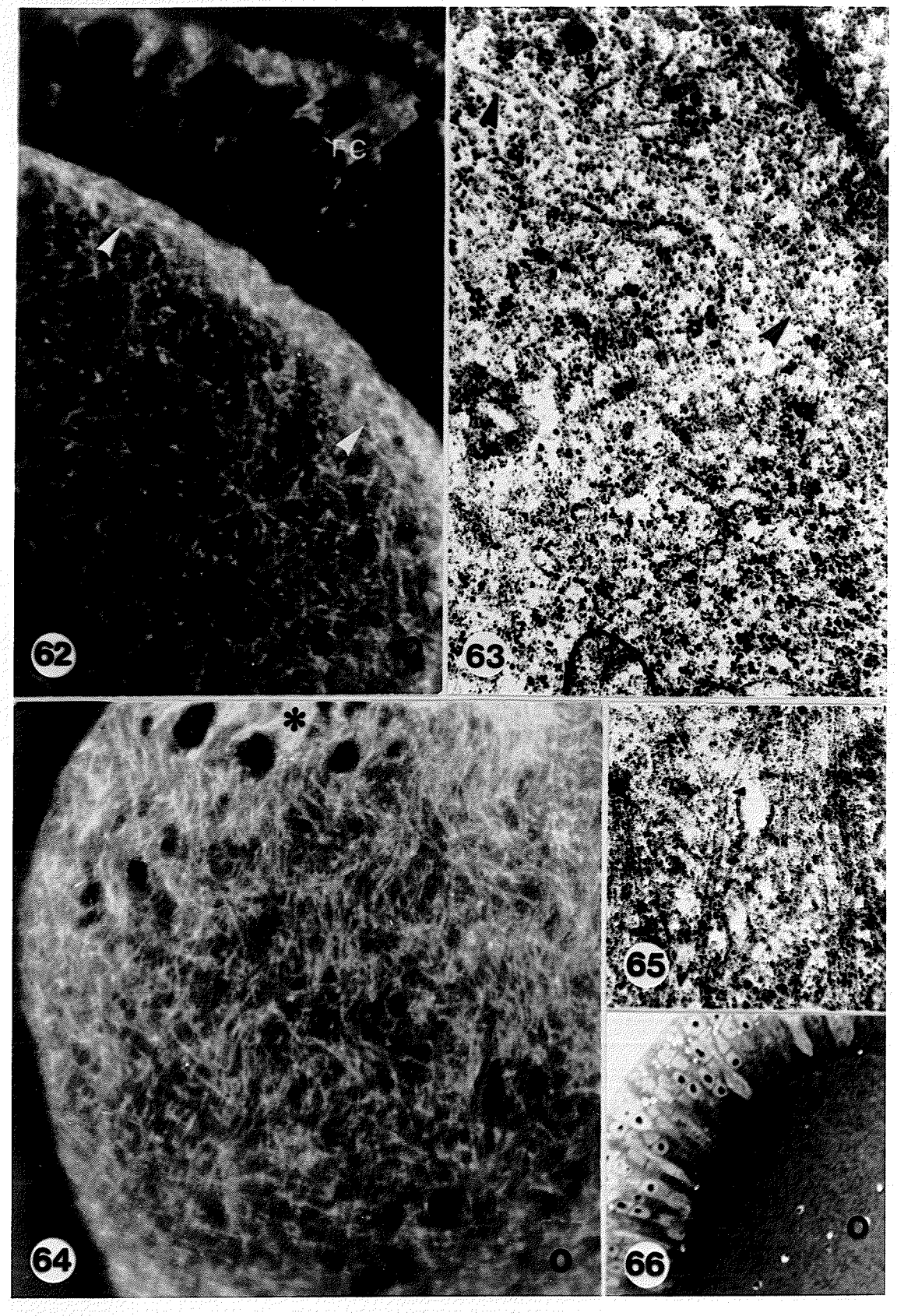
FC
62
63
64
65
66
O
O

PLATE 14

Dynamics of the Microtubule Cytoskeleton
Early Vitellogenesis

Figure 67 — Immunofluorescence micrograph of the anterior region of an early vitellogenic follicle. Note the entry of the trophic cord microtubules into the oocyte and their presence in the cortex (arrowheads) X1,200

Figure 68 — Immunofluorescence micrograph shows the well defined band of tubulin fluorescence in the posterior region of the oocyte cortex (arrows). X550

Figure 69 — TEM micrograph of microtubules in the cortex. X38,650

Figure 70 — Immunofluorescence micrograph of the anterior and lateral regions of the oocyte cortex. Note the brilliant staining of the anterior region (arrowheads) verses the dispersed staining of the lateral cortex (arrows). X850

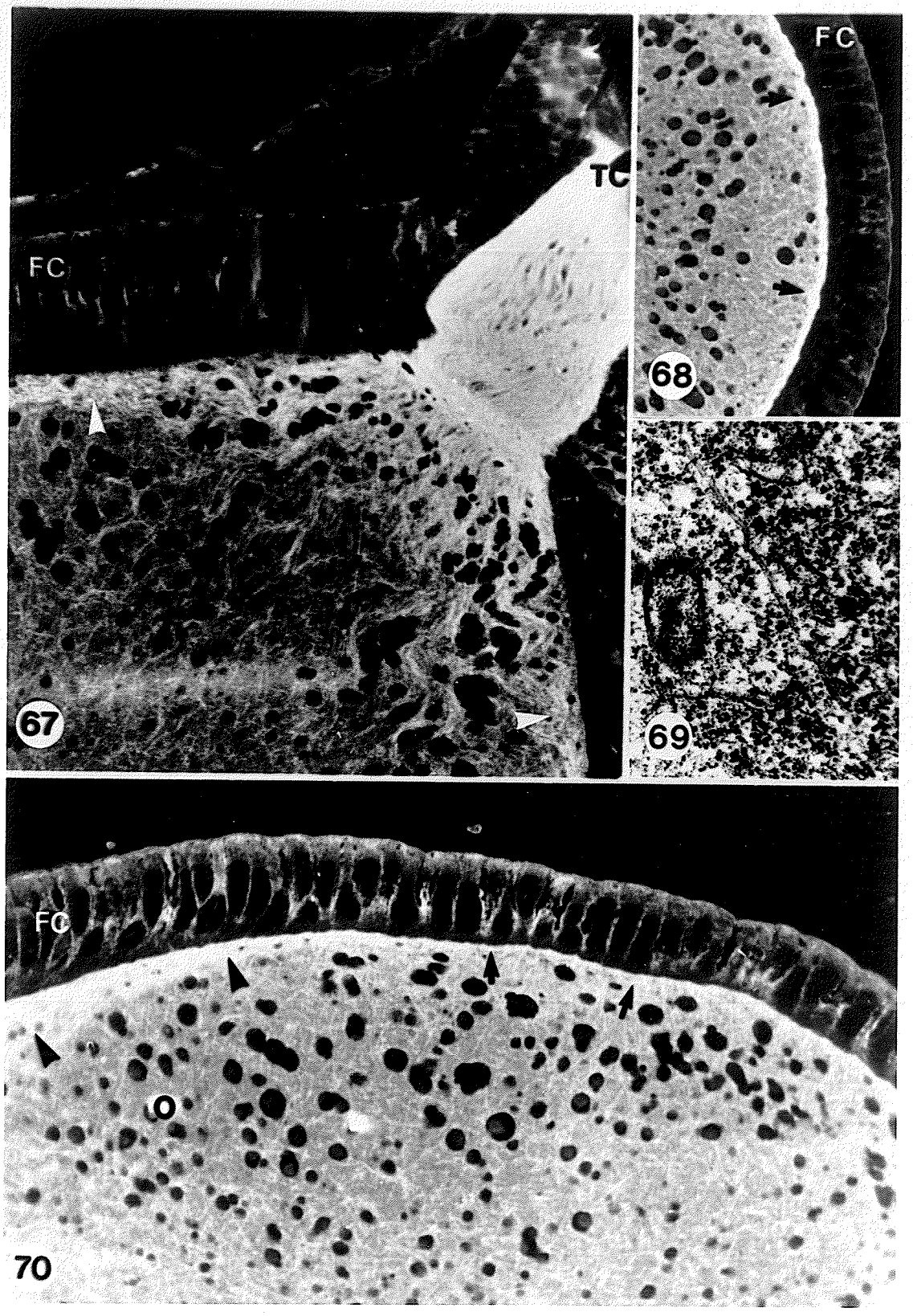
FC
TC
67
FC
68
69
FC
O
70

PLATE 15

Dynamics of the Microtubules Cytoskeleton
Late Vitellogenesis

Figure 71	Brightfield micrograph of the lateral cortex, illustrating the intercellular spaces and the abundance of yolk spheres. Arrowheads denotes follicle cell processes. X650
Figure 72	Immunofluorescence micrograph through the lateral region of the follicle illustrating the faint tubulin staining pattern that persists throughout vitellogenesis (arrowheads). X1,250
Figure 73	A survey SEM micrograph of a cleaved vitellogenic oocyte displaying its overall features and the abundance of yolk spheres. X1,000
Figures 74, 75 & 76	TEM micrographs of the lateral cortex showing the abundance of microvilli (MV), intercellular spaces, and the presence of microtubules in the cortex (arrowheads). Fig. 75 reveals a cross sectional view and Fig. 76 a longitudinal view. X10,300, X52,850, X72,150

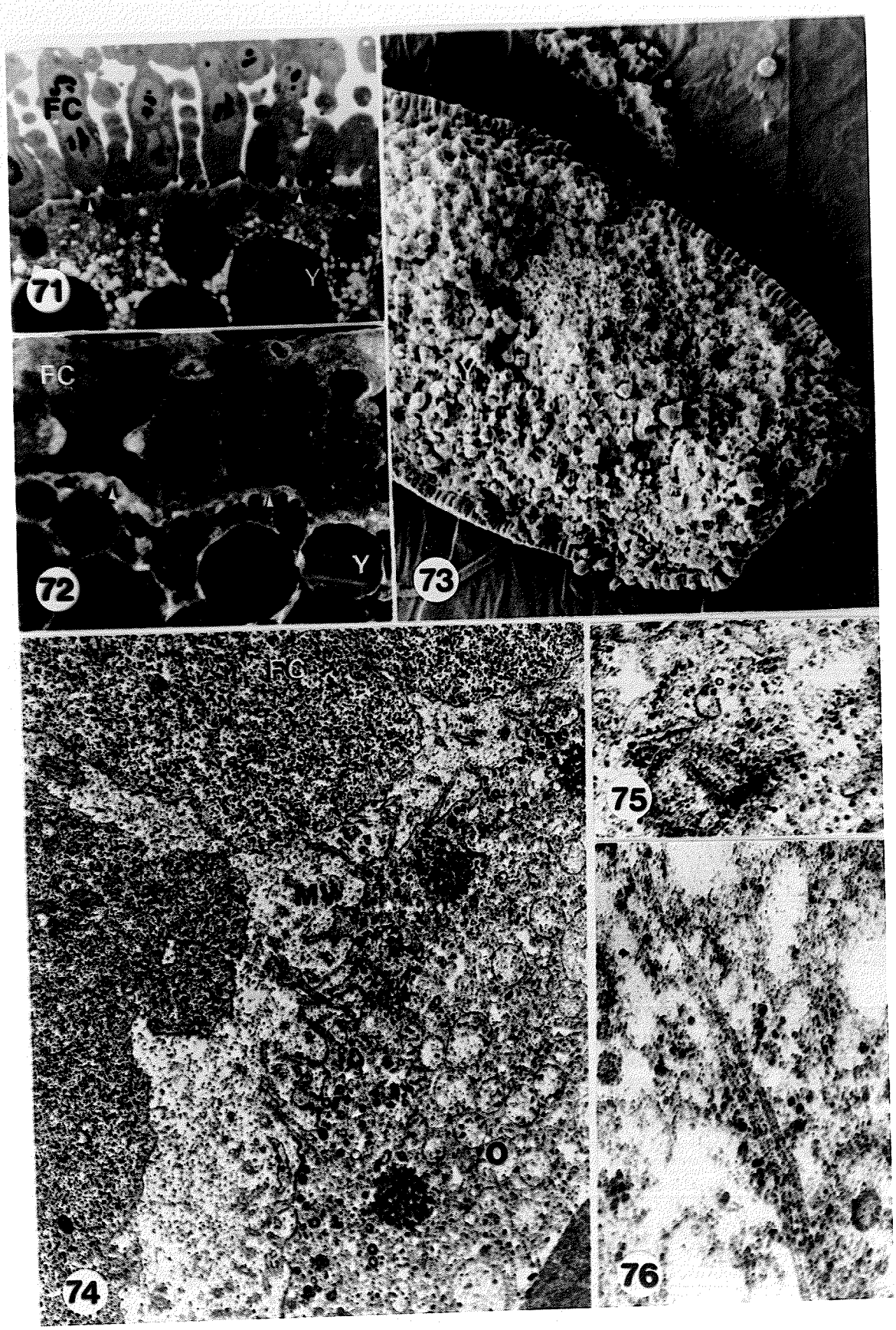
FC
Y
71
FC
Y
72
73
FC
74
75
76

PLATE 16

Biochemical Analysis

Figure 77 Silver stained polyacryamide gel. Lane 1, BioRad prestained MW markers; lanes 2, 3 & 4, Rhodnius ovary homogenate; lanes 5 & 8 purified actin preparation; lane 6, day 1 Rhodnius embryo homogenate; and lane 7, day 7 Rhodnius embryo homogenate. X1

Figure 78 Western Blot of a polyacrylamide gel stained for F-actin. Lane A, purified actin sample; lane B, day 1 Rhodnius embryo; lane C, day 7 Rhodnius embryo; and lane D, Rhodnius ovary homogenate. X1


77
66
45
30
77
78
1 2 3 4 5 6 7 8 A B C D

DISCUSSION

GENERAL FEATURES OF THE OOCYTE CORTEX

During previtellogenesis the oocyte of Rhodnius prolixus appears to be a receptacle for materials synthesized by the nurse cells. Thus, the synthetic machinery of the oocyte is not well developed. There are few Golgi complexes in the ooplasm which are small and have flattened cisternae. They are similar in appearance to those found in the cockroach, Periplaneta americana (Anderson, 1969). In Periplaneta, the Golgi complexes remain inactive throughout oogenesis (Anderson, 1969). Mahowald (1972) has found that no significant ultrastructural changes occur in previtellogenic oocytes of Drosophila mitochondria and free ribosomes are common, as in Rhodnius but unlike Rhodnius, rough endoplasmic reticulum (RER) is sparse in Drosophila (Mahowald, 1972). In Periplaneta oocytes, RER is also absent during all stages of oogenesis (Anderson, 1964). Smooth endoplasmic reticulum is sparsely distributed throughout the deeper regions of the cortex in Rhodnius prolixus, while RER is quite abundant throughout the cytoplasm. RER is

found in two distinct forms in Rhodnius prolixus. The first is the most commonly found in eukaryotic cells. This type of RER is abundant throughout the ooplasm. The nurse cells synthesize many messenger RNAs, including those for tubulin, actin, clathrin and other major proteins (Huebner, 1984). Thus, the oocyte must have the means to translate these mRNAs when needed. The second type of RER found appears to be a novel form of RER packaging. Zissler and Sander (1982) describe three different configurations of RER in Smittia eggs. The unusual form of RER found in Rhodnius does not fit into any of the three categories that they describe. The ER stacks are closely linked together by what appears to be fibrous material, forming large RER whorls throughout the deeper regions of the cortex. This form of RER packaging limits the cisternal area that is available for ribosomes to be attached, and thus limits potential translation. These whorls are not found in the later stages of oogenesis, thus, it is possible that they have 'unwound' so that translation may proceed at a higher level of activity. The ooplasm is abundant with free ribosomes, they are rarely found as polyribosomes. However, in a few cases spiral polyribosomes were located in the ooplasm. They

appeared in tangential sections of the RER whorls, indicating that the ribosomes on the free cisternae are actively translating messages. The function of this novel RER configuration remains elusive and requires further investigation.

Immediately prior to vitellogenesis, annulate lamellae appear at the boundary of the cortex. In Rana pipiens the annulate lamellae move towards the cortex where they subsequently fragment (Imoh, 1982). In the dragon fly, Libellula pulchella, annulate lamellae are found near the nuclear envelope during early oogenesis and near the cortex in the later stages of oogenesis (Kessel and Beams, 1969). Although fragmentation of annulate lamellae was not observed in Rhodnius, it is possible as they were only observed occasionally during the later stages of oogenesis. The precise role of annulate lamellae in the oocyte is not yet defined. Huebner and Anderson (1972b) suggest that the annulate lamellae in Rhodnius function in the storage of nuclear precursor material that is needed for blastoderm formation; while Imoh (1982) suggests that in the newt, Cynops, the material on the annulate lamellae is poly A-mRNA.

During previtellogenesis, while the cortex is differentiating the cytoskeletal components, the membrane related machinery essential to the whole process of vitellogenesis develops. The appearance of clathrin coated plasma membrane patches and pits and clathrin coated vesicles thereby also become integral parts of the oocyte cortex. Uncoated vesicles were also observed, as previously noted by Telfer et al (1982). The coated vesicles were sometimes seen in close association with microtubules. However, I was unable to determine from my observations whether or not they were linked. It is also possible that clathrin coated pits are associated with microfilaments. The abundance of microfilaments that form the microvillar core suggests that they may be involved in shuttling the vesicles to and from the oolemma.

During vitellogenesis, the amount of microvilli on the lateral surface increases dramatically to accommodate the high rate of membrane turnover during endocytosis of yolk proteins. These microvilli all have a microfilament core that provides rigidity. The apical and posterior follicle cells do not separate, and there are correspondingly fewer microvilli, and microfilaments.

Once vitellogenesis is complete, the follicle cells secrete the acellular chorion. The follicle cells that produce the micropyles in the chorion form a distinct band that is evident during vitellogenesis. The opposing oolemma is also distinct from the rest of the oolemma in that the underlying cytoskeleton is modified. This is reflected in the form of the microvilli that cover this region. They appear somewhat similar to the spiral microvilli observed by Schroeder (1982) in the sea anemone Tealia crassicornis, in that the microvilli are clumped together and are closely associated with one another. The formation of these microvilli reflects the follicular projections into the oolemma and possibly reflects modification of the oocyte cytoskeleton for ease of sperm penetration and facilitation of sperm pronucleus migration towards the oocyte pronucleus.

INTEGRATION OF METHODS

The use of different approaches; buffer systems, scanning and transmission electron microscopy, immunofluorescence and rhodamine phalloidin staining capitalizes on the advantages of each technique and

minimizes the disadvantages. Thus, allowing one to reveal the dynamics of the cortex during oogenesis.

The follicle cells were removed so that the oocyte surface could be visualized. This procedure is somewhat harsh in that the follicle is kept in saline for an extended time while the follicle cells are mechanically removed. Therefore, to use this method alone may have resulted in inaccurate characterization of the surface topography. In addition, SEM does not permit positive identification of cytoskeletal elements in the extracted preparations. The cytoplasm of the unextracted preparations has a homogeneous appearance so one cannot distinguish any elements. However, under stringent conditions and in combination with rhodamine phalloidin staining and TEM, SEM of whole mounts does provide an excellent method by which to view the changes in the surface topography of the oocyte highlighting regional differences.

Whole mount preparations of SEM and rhodamine phalloidin were used in contrast to the isolated cortex in order to compare surface patterns and to attribute staining to either the ooctye cortex or to the entire ooplasm. The comparison of these two methods permits assessment of the validity of each.

Indirect immunofluorescent staining of DGD embedded material is a new technique (Valdimarsson and Huebner, 1989). The DGD is easily removed from the sections and the antigenicity is preserved. Immunofluorescence is a practical tool for pattern visualization in large cells such as Rhodnius prolixus and it permits an overall assessment of protein distribution. The Anti-tubulin antibody used binds to both tubulin subunits and polymers. This presents a method by which to examine the total tubulin within the oocyte. Microtubule analysis by being used in conjunction with TEM, allowed for the positive identification of microtubules and their distribution within the cortex.

The Anti-actin antibody used also bound both the polymerized and unpolymerized forms of actin. Thus, the pattern of F-actin was complemented by the use TEM and rhodamine phalloidin specific staining of whole mounts and isolated cortices. Analysis of microfilaments in the oocyte cortex was aided by the removal of the follicular epithelium. The follicle cells project microfilament containing microvilli into the oocyte cortex. Thus, when examining Anti-actin stained DGD sections, some of the fluorescence had to

be attributed to G-actin and follicle cell microfilaments. The removal of the follicle cells assured me that the staining observed was due to the oocyte cortex alone. TEM distinguished between oocyte and follicle cell microfilaments.

DYNAMICS OF THE MICROFILAMENT CYTOSKELETON

Previtellogenesis

Small previtellogenic oocytes, <150 uM, do not appear to have a discernible microfilament cytoskeleton. They have just begun to acquire materials and organelles from the nurse cells and presumably have not yet accumulated actin or actin mRNA. In oocytes 150-350 uM in length, not only are microfilaments associated with membrane specializations, they also form an elaborate network in the underlying cortex. The oocyte has a great store of G-actin. This is apparent by the amount of Anti-actin staining and by the *in vitro* elongation of microvilli. The elongation of microvilli can be induced by leaving the denuded oocyte in saline for an extended time period (see also Huebner, 1984). This can be observed by SEM of such follicles. When one shears these

elongated microvilli from the oocyte, the underlying cortex is displayed. SEM micrographs reveal a tightly woven cytoskeletal network underneath these microvilli that is able to maintain its integrity and withstand high shearing forces. This also shows that the oocyte has the potential to form a greater number of microfilaments than are observed *in vivo*. The existing microvilli elongate and new microvilli appear on the surface. Thus, the *in situ* conditions must somehow be regulated so that some of the actin remains in the unpolymerized state. This could be accomplished by the presence of actin binding proteins in combination with microenvironments of increased or decreased pH which causes either the polymerization or depolymerization of actin, depending upon the conditions in the rest of the ooplasm (Carron and Longo, 1982 and Begg *et al*, 1982). In the intestinal brush border, calmodulin and villin are associated with the microfilament core of the microvilli (Glenney *et al*., 1980). Glenney *et al*., (1980) suggested that villin acts as a calcium sensitive regulator of microfilament assembly and disassembly, while calmodulin acts as a buffer modulating free calcium concentration. "Actin bundles are thought to support the microvilli and have a role

in the dynamic changes which they undergo" (Warn and Magrath, 1983). The microfilament core may also serve as a nucleation site for the polymerization of G-actin stores (Henson and Begg, 1988). The appearance of cortical microfilaments correlates well with the structural changes of the oocyte surface.

As previously noted by Huebner (1984) there is an abrupt transition from a smooth to a microvilli covered surface where the trophic cord enters the oocyte. The anti-actin staining of DGD sections clearly shows the cortical actin concentration correlates precisely with the elaboration of the microvillar surface.

Vitellogenesis

During vitellogenesis, there is an increase in microvilli covering the lateral surface of the oocyte. These microvilli have a microfilament core. The formation of microfilament bundles is not necessary for microvillar elongation, however, they are required for support (Begg *et al.*, 1982). The microfilament cores found in *Rhodnius* extend deep into the cortex, unlike the microfilament cores in the unfertilized sea urchin oocytes which are short (Henson and Begg, 1988).

Perhaps in Rhodnius this extension is required for increased support for the microvilli and for the transport of coated vesicles into the deeper regions of the cortex. .

Presently nothing is known about the interaction of actin filaments and the plasma membrane in Rhodnius oocytes. This is most likely mediated by actin binding proteins, however, it is also possible that actin interacts directly with the plasma membrane lipids (Rioux and Gicquard, 1985). Also, the significance of the high molecular weight of actin in Rhodnius oocytes and embryos, is as yet unknown. For example, why in Rhodnius is such a highly conserved protein so dramatically different in weight.

The significant amount of microfilaments in the lateral cortex excludes all organelles except for clathrin coated and uncoated vesicles and ribosomes from the cortex. This presumably provides for a local environment in which intense activity in pinocytotic vesicle formation and shuffling becomes possible. The cortex must therefore provide not only a physical, mechanical and structural framework, but also it must reflect the intense dynamic activity that occurs there throughout much of oogenesis and early embroyogenesis.

Warn and MaGrath (1983) and Warn et al., (1985) have shown that the elaborate microfilament network in early Drosophila embryos contracts simultaneously "causing the extension of cell membranes and hence the cellularization of the blastoderm". The organization of the microfilament in oogenesis may also control the spatial distribution of organelles and thus establish cytoplasmic localization (Shimizu, 1988).

The influence of the follicle cells on the adjacent oolemma is significant. The shape of the micropyle producing follicle cells influences the oolemma in the anterior region of the oocyte as discussed earlier. However, the discrete pattern of microfilament containing microvilli is more dramatic in the lateral regions of the oocyte. The microvilli are somewhat longer in regions that are adjacent to the spaces in between follicle cells, presumably exposing more membrane receptors to the yolk proteins in the hemolymph. The underlying microfilament cytoskeleton must somehow be influenced to undergo actin polymerization at localized positions.

DYNAMICS OF THE MICROTUBULE CYTOSKELETON

Previtellogenesis

In order to understand the role mircotubules play in cell cleavage, chromosome, yolk sphere and mitochondrial movement etc., it is important to know the distribution and rearrangements of microtubules in the entire egg (Hollenbeck and Cande, 1985). Until recently there was little evidence in the literature to suspect that unfertilized eggs contained microtubules. They were thought to contain a large pool, 0.4% of the total protein in sea urchin eggs, of tubulin subunits (Raff et al, 1975). Then at fertilization an increase in pH results in the polymerization of these tubulin subunits in sea urchins (Schatten et al, 1985). The presence of microtubules in insect oocytes has been reported by Huebner and Anderson (1972b) and Mahowald (1972). Mahowald (1972) observes that microtubules are sparsely scattered throughout the cortex of Drosophila oocytes during all stages of oogenesis. They radiate away from the cortex suggesting a possible role in the movement of yolk spheres (Mahowald, 1972). Bier has reported that mircotubules function in yolk movement (Mahowald, 1972). In fertilized sea urchin eggs, the

microtubules are also oriented perpendicular to the surface of the oocyte (Harris et al, 1980). They propose that these microtubules function in the transport of the pronuclei to the egg center (Harris et al, 1980). Telfer and Anderson (1968) do not describe microtubules in their study of Cecropia oocytes. If the movement of yolk spheres is the principle function of microtubules in insect eggs, then perhaps their absence is explicable by the fact that in Cecropia yolk spheres do not move (Mahowald, 1972). "Ultrastructural studies, however, are difficult to interpret unless these structural observations can be correlated with various functional and molecular parameters" (Mahowald, 1972).

The tubulin pattern obtained by Anti-tubulin staining of small previtellogenic Rhodnius oocytes reveals short strands throughout the entire oocyte. There is no evidence of a defined microtubule cortex at this stage.

During mid-previtellogenesis microtubules are observed by TEM and immunofluorescence in the cortex of the oocyte indicating that a distinct cortical microtubule cytoskeleton has formed. The abundance of tubulin in the previtellogenic cortex is particularly

well displayed using Anti-tubulin staining of a DGD section through the cortex. The microtubules presumably function in a structural role and possibly in the transport of organelles in the ooplasm during this stage of oogenesis.

Vitellogenesis

Be early vitellogenesis when the lateral follicle cells have begun to separate, the cortical microtubules in the anterior region still remain distinct. They are probably extensions of the trophic cord microtubules deeper into the oocyte so to facilitate the transport of the nurse cell derived materials further into the oocyte. The integrity of these microtubule bundles requires further examination, as to the nature of the link between adjacent microtubules. Haimo et al., (1979) have suggested that dynein forms cross bridges between microtubules so that they form bundles. Also the function of the well defined microtubule band in the posterior region of the oocyte is unknown. In contrast, the abundance of microtubules in the lateral cortex at this stage diminishes significantly. This situation corresponds with the onset of vitellogenesis

and is maintained throughout vitellogenic growth. The few scattered microtubules are oriented parallel to the surface suggesting that they cannot play a significant role in the transport of yolk spheres or clathrin coated vesicles in the cortex. Tucker and Meats (1976) studied microtubule organization in the panoistic ovaries of Periplaneta and the polytrophic ovaries of Heteropeza. They reported that oocyte shape was due to the microtubule cytoskeleton of the surrounding follicle cells. This was also reported by Went (1978) since these oocytes displayed very few microtubules which were randomly oriented. In Rhodnius, the follicle cells also have an elaborate microtubule cytoskeleton (Watson and Huebner, 1986) suggesting that the follicle cells have a role in determining oocyte shape. However, the abundance and orientation of the microtubules in the posterior oocyte cortex suggests that they also have a role in determining oocyte shape.

The diminution of the lateral microtubules in the early stages of vitellogenesis presumably is essential to allow for less obstruction due to the increased traffic of coated and uncoated vesicles and membrane recycling. This is a very dynamic region of the cortex, so the microtubule reduction may also reflect

the need for decreased structural stability in this region which is constantly undergoing membrane rearrangements due to the amount of pinocytotic activity. It is also possible that this may reflect a local environment of increased calcium concentration which would cause the depolymerization of microtubules (Schliwa and van Blerkom, 1981).

SUMMARY

A discernable microfilament and microtubule cytoskeleton does not develop until mid-previtellogenesis. By late previtellogenesis the oocyte cortex has a tightly woven network of microfilaments and microtubules, excluding most organelles from the cortex. During vitellogenesis the lateral microtubule cytoskeleton diminishes, while the abundance of microfilament containing microvilli increases. The cortex contains many coated vesicles and the cytoplasm accumulates numerous yolk spheres. The dynamics of the oocyte cortical cytoskeleton are reflected in the complexity of the membrane changes of the oocyte surface.

This research provides a background for many avenues of study, such as, the exact nature of the interactions between the plasma membrane and the microfilaments, as well as the interactions between microfilaments and microtubules. I attempted to establish the presence of an intermediate filament cytoskeleton, however, my results were nonconclusive. I used antibodies to various intermediate filaments, none of which bound to DGD sections of Rhodnius oocytes. This negative result can be interpreted in three ways. Firstly, fixation (3% PFA, 0.5% GTA, 1mM GTP in PHEM) conditions caused the loss of intermediate filament antigenicity. Godsave et al (1984b) and Franke et al (1978) report that aldehyde fixation causes the loss of intermediate filament antigenicity. Secondly, the intermediate filaments in Rhodnius may not contain a region that is homologous to the antibodies used and therefore no binding occurred. Thirdly, Rhodnius does not contain intermediate filaments. The latter possibility would be quite unlikely since intermediate filaments of some form are found in most germ tissue. The first and second explanations are the most probable. It is most likely a problem with antibody specificity since the

glutaraldehyde concentration used was very low.

Preliminary in situ hybridization studies were also carried out. These results were also inconclusive. The number of background grains was high and experimental and control hybridization patterns were conflicting. Some control slides showed no specific binding over the tissue while others displayed high number of grains over the follicular epithelium. Experimental slides did not have specific binding to the nurse cells which are known to be actively synthesizing poly(A+) mRNAs (Capco and Jeffery, 1979). Thus, this requires further investigation into the conditions which would facilitate the hybridization the poly(U) probe.

LITERATURE CITED

Anderson, E. 1964. Oocyte differentiation and vitellogenesis in the roach Periplaneta americana. J Cell Biol. 20, 131-155.

Anderson, E. 1969. Oogenesis in the cockroach, Periplaneta americana, with special references to the specialization of the oolemma and the fate of coated vesicles. J. Microscopie. 8, 721--738.

Anderson, W. and R. Ellis. 1965. Ultrastructure of Trypanosoma lewisi flagelluum, microtubules and the kinetoplast. J. Protozool. 12, 484-499.

Bag, J. and S. Pramanik. 1987. Attachment of mRNA to the cytoskeletal framework and translational control of gene expression in rat L6 muscle cells. Biochem Cell Biol. 65, 565-575.

Begg, D., L. Rebhun and H. Hyatt. 1982. Structural organization of actin in the sea urchin egg cortex: microvillar elongation in the absence of actin filament bundle formation. J Cell Biol. 93, 24-32.

Bergen, L. and G. Borisy. 1980. Head-to-tail polymerization of microtubules in vitro. Electron microscope analysis of seeded assembly. J. Cell Biol. 84, 141-150.

Bestor, T. and G. Schatten. 1981. Anti-tubulin immunofluorescence microscopy of microtubules present during pronuclear movements of sea urchin fertilization. Dev. Biol. 88, 80-97.

Bond, M. and A.V. Somylo. 1982. Dense bodies and actin polarity in vertebrate smooth muscle. J. Cell Biol. 95, 403-413.

Bonhag, P. 1955. Histochemical studies of the ovarian nurse tissues and oocytes of the milkweed bug, Oncopeltus fasciatus (Dallas). J. Morph. 96, 381-440.

Burgess, D. 1977. Polymerized actin in the isolated sea urchin egg cortex. J Cell Biol. 75(2), 254a.

Burgess, D. and T. Schroeder. 1979. The cytoskeleton and cytomusculature in embryogenesis- an overview. Meth. Archiev. exp. Pathol. 8,171-189.

Capco, D. and W. Jeffery. 1979. Origin and spatial distribution of maternal messenger RNA during oogenesis of an insect, Oncopeltus fasciatus. J. Cell Sci. 39, 63-76.

Capco, D. and R. McGaughey. 1986. Cytoskeletal reorganization during early mammalian development: analysis using embeddment-free sections. Dev. Biol. 115, 446-458.

Capco, D., G. Krochmalnic and S. Penman. 1984. A new method of preparing embeddment-free sections for transmission electron microscopy: applications to the cytoskeletal framework and other three-dimensional networks. J. Cell Biol. 98, 1878-1885

Carron, C. and F. Longo. 1982. Relation of cytoplasmic alkalinization to the microvillar elongation and microfilament formation in the sea urchin egg. Dev. Biol. 89, 128-137.

Chandler, D. and J. Heuser. 1981. Postfertilization growth of microvilli in the sea urchin egg: new views from eggs that have been quick-frozen, freeze-fractured, and deeply etched. Dev. Biol. 82, 393-400.

Cleveland, D. 1983. The tubulins: from DNA to RNA to protein and back again. Cell 34, 330-332.

Coffe, G., G. Foucault, M. Soyer, F. DeBilly and J. Pudles. 1982. State of actin during the cycle of cohesiveness of the cytoplasm in parthenogenetically activated sea urchin eggs. Exp. Cell Res. 142, 365-372.

Colman, A., J. Morser, C. Lane, J. Besley, C. Wylie and G. Valle. 1981. Fate of secretory proteins trapped in oocytes of Xenopus laevis by disruption of the cytoskeleton or by imbalanced subunit synthesis. J. Cell Biol. 91, 770-780.

Colombo, R., P. Benedusi and G. Valle. 1981. Actin in Xenopus development: Indirect immunofluorescence study of actin localization. Differentiation. 20, 45-51.

Davidson, E. 1986. Gene Activity in Early Development. Third Edition. Academic Press, Inc., Orlando. 670p.

Ducibella, T., T. Ukena, M. Karnovsky and E. Anderson. 1977. Changes in cell shape and cortical cytoplasmic organization during early embryogenesis in the preimplantation mouse embryo. J. Cell Biol. 74, 153-167.

Dumont, J. and R. Wallace. 1972. The effects of vinblastine on isolated Xenopus oocytes. J. Cell Biol. 53, 605-610.

Eddy, E. and B. Shapiro. 1976. Changes in the topography of the sea urchin egg after fertilization. J. Cell Biol. 71, 35-48.

Elinson, R. and M. Manes. 1978. Morphology of the site of sperm entry in the frog egg. Dev. Biol. 63, 67-67.

Franke, W., P. Rathke, E. Seib, M. Trendelenburg, M. Osborn and K. Weber. 1976. Distribution and mode of arrangement of microfilamentous structures and actin in the cortex of the amphibian oocyte. Cytobiologie. 14, 111-130.

Franke, W., E. Schmid, M. Osborn and K. Weber. 1978. Different intermediate-sized filaments distinguished by immunofluorescence microscopy. Proc. Natl. Acad. Sci. USA. 75(10), 5034-5038.

Franz, J., L. Gall, M. Williams, B. Picheral and W. Franke. 1983. Intermediate-size filaments in a germ cell: expression of cytokeratins in oocytes and eggs of the frog Xenopus. Proc. Natl. Acad. Sci. USA. 80, 6254-6258.

Foucault, G., N. Raymond and J. Pudles. 1987. Cytoskeleton of the unfertilized sea urchin egg. Biology of the Cell. 60, 63-70.

Gall, L., B. Picheral and P. Gounon. 1983. Cytochemical evidence for the presence of intermediate filaments and microfilaments in the egg of Xenopus laevis. Biol. Cell. 47, 331-342.

Gilbert, S. 1988. Developmental Biology. Sinuar Ass. Inc. Massachusetts. pp. 843.

Glenney, J.A. Bretscher and K. Weber. 1980. Calcium control of the intestinal microvillus cytoskeleton: its implications for the regulation of microfilament organizations. Proc. Natl. Acad. Sci. USA 77(11), 6458-6462.

Godsave, S., C. Wylie, E. Lane and B. Anterton. 1984a. Intermediate filaments in the Xenopus oocyte: the appearance and distribution of cytokeratin-containing filament. J. Exp. embryol. Morph. 83, 157-167.

Godsave, S. B. Anterton, J. Heasman and C. Wylie. 1984b. Oocytes and early embryos of Xenopus laevis contain intermediate filaments which react with anti-mammalian vimentin antibodies. J. Exp. embryol. Morph. 83, 169-187.

Gutzeit, H. and E. Huebner. 1986. Comparison of microfilament patterns in nurse cells of different insects with polytrophic and telotrophic ovaries. J. Exp. embryol. Morph. 93, 291-301.

Haimo, L., B. Telzer and J. Rosenbaum. 1979. Dynein binds to and cross bridges cytoplasmic microtubules. Proc. Natl. Acad. Sci. USA 76(11), 5759-5763.

Handel, M. and L. Roth. 1971. Cell shape and morphology of the neural tube: implications for microtubule function. Dev. Biol. 25,78-95.

Harris, H. 1987. Microfilament dynamics. Few answers but many questions. Nature. 330, 310-311.

Harris, P., M. Osborn and K. Weber. 1980. A spiral array of microtubules in the fertilized sea urchin egg cortex examined by indirect immunofluorescence and electron microscopy. Exp. Cell Res. 126, 227-236.

Hayden, J. and R.D. Allen. 1984. Detection of single microtubules in living cells: particle transport can occur in both directions along the same microtubule. J. Cell Biol. 99, 1785-1793.

Heggeness, M., M. Simon and S. Singer. 1978. Association of mitochondria with microtubules in cultured cells. Proc. Natl. Acad. Sci. USA. 75(8), 3863-3866.

Heidemann, S., M. Hamburg, J. Balasz and S. Lindley. 1985. Microtubules in immature oocytes of Xenopus laevis. J. Cell Sci. 77, 129-141.

Henson, H. and D. Begg. 1988. Filamentous actin in the unfertilized sea urchin egg cortex. Dev. Biol. 127, 338-348.

Hollenbeck, P. and W.Z. Cande. 1985. Microtubule distribution and reorganization in the first cell cycle of fertilized eggs of Lytechinus pictus. Eur. J. Cell Biol. 37, 140-148.

Hopkins, C. and P. King. 1966. An electron-microscopical and histochemical study of the oocyte periphery in Bombus terrestris during vitellogenesis. J. Cell Sci. 1, 201-216.

Howe, G. and J. Hershey. 1984. Translational initiation factor and ribosome association with the cytoskeletal framework fraction from HeLa cells. Cell. 37, 85-93.

Huebner, E. 1984. The ultrastructure and development of the telotrophic ovary. In Insect Ultrastructure and Development Vol. 2. R.C. King and H. Akai (Eds). Plenum Press. New York. pp. 3-48.

Huebner, E. and E. Anderson. 1970. The effects of vinblastine sulfate on the microtubular organization of the ovary of Rhodnius prolixus. J. Cell Biol. 46, 191-198.

Huebner, E. and E. Anderson. 1972a. A cytological study of the ovary of Rhodnius prolixus I. The ontogeny of the follicular epithelium. J. Morph. 136, 495-504.

Huebner, E. and E. Anderson. 1972b. A cytological study of the ovary of Rhodnius prolixus II. Oocyte differentiation. J. Morph. 137, 285-416.

Huebner, E. and E. Anderson. 1972c. A cytological study of the ovary of Rhodnius prolixus III. Cytoarchitecture and development of the trophic chamber. J. Morph. 138, 1-40.

Huebner, E. and R. Dohmen. 1988. The polarized topographical organization of the cortical cytoskeleton in early molluse embryos. 4th International Congress of Cell Biology. p. 171 Abs.

Huebner, E. and H. Injeyan. 1981. Follicular modulation during oocyte development in an insect: formation and modification of septate and gap junctions. Dev. Biol. 83, 101-113.

Imhof, B., U, Marti, K. Boller, H. Frank and W. Birchmeier. 1983. Association between coated vesicles and microtubules. Exp. Cell Res. 145, 199-207.

Imoh, H, 1982. Behaviour of annulate lamellae during the maturation of oocytes in the newt, Cynops pyrrhogaster. J. Embryol. Exp. Morph. 70, 153-169.

Jackson, B., C. Grund, E. Schmid, K. Burki, W. Franke and K. Illmensee. 1980. Formation of cytoskeletal elements during mouse embryogenesis. Intermediate filaments of the cytokeratin type and desmosomes in preimplantation embryos. Differentiation. 17, 161-179.

Jeffery, W. 1983. Messenger RNA localization and cytoskeletal domains in Ascidian embryos. In Time, Space and Patterns in Embryonic Development. Alan R. Liss Inc. New York. pp. 241-259.

Jeffery, W., J. Speksnijder, B. Swalla and J. Venuti. 1986. Mechanism of maternal mRNA localization in Chaetopterus eggs. Adv. Invert. Reprod. 4. 229-241.

Jessus, C., C. Thibier and R. Ozon. 1987. Levels of microtubules during the meiotic maturation of the Xenopus oocyte. J. Cell Sci. 87, 705-712.

Jessus, C., D. Huchon and R. Ozon. 1986. Distribution of microtubules during the breakdown of the nuclear envelope of the Xenopus oocyte: an immunocytochemical study. Biol. Cell. 56, 113-120.

Johnson, L., M. Walsh and L. Chen. 1980. Localization of mitochondria in living cells with rhodamine 123. Pro. Natl. Acad. Sci. USA. 77(2), 990-994.

Juurlink, B. and R. Dell. 1980. A simple method for producing fine stainless steel dissecting needles and microscapels. Experientia. 36, 1335.

Kane, R. 1986. TAME stabilizes the cortex and mitotic apparatus of the sea urchin egg during isolation. Exp. Cell Res. 162, 494-506.

Karnovsky, M. 1965. A formaldehyde-glutaraldehyde fixative of high osmolality for use in electron microscopy. J. Cell Biol. 27, 137a.

Katsuma, Y., S. Swierenga, N. Marceau and S. French. 1987. Connections to intermediate filaments with the nuclear lamina and the cell periphery. Biol. of Cell. 59, 193-204.

Kessel, R. and H. Beams. 1969. Annulate lamellae and 'yolk nuclei' in oocytes of the dragonfly, Libellula pulchella. J. Cell. Biol. 42, 185-201.

Klymkowsky, M., L. Maynell and A. Polson. 1987. Polar asymmetry in the organization of the cortical cytokeratin system of Xenopus laevis oocytes and embryos. Dev. 100, 543-557.

Korn, E. 1982. Actin polymerization and its regulation by proteins from nonmuscle cells. Physiological Reviews. 62, 672-737.

Lazarides, E. 1980. Intermediate filaments as mechanical integrators of cellular space. Nature. 283, 249-256.

Lenk, R. and S. Penman. 1979. The cytoskeletal framework and polio virus metabolism. Cell. 16, 289-301.

Lenk, R., L. Ransom, Y. Kaufmann and S. Penman. 1977. A cytoskeletal structure with associated polyribosomes obtained from HeLa cells. Cell. 10, 67-78.

Lessman, C. 1987. Germinal vesicle migration and dissolution in Rana pipiens oocytes: effects of steriods and microtubule poisons. Cell Differentiation. 20, 239-252.

Longo, F. 1980. Organization of microfilaments in sea urchin (Arbacia punctulata) eggs at fertilization: effects of cytochalasin B. Dev. Biol. 74, 422-433.

Longo, F. 1985. Fine structure of the mammalian egg cortex. Am. J. Anat. 174, 303-315.

Longo, F. 1986. Surface changes at fertilization: integration of sea urchin (Arbacia punctulata) sperm and oocyte plasma membranes. Dev. Biol. 116, 143-159.

Longo, F. 1987. Actin-plasma membrane association in mouse eggs and oocytes. J. Exp. Zool. 243, 299-309.

MacGregor, H. and H. Stebbings. 1970. A massive system of microtubules associated with cytoplasmic movement in telotrophic ovarioles. J. Cell Sci. 6, 431-449.

Maddrell, S. 1969. Secretion by the Malphigian tubules of Rhodnius. The movements of ions and water. J. Exp. Biol. 51, 71-97.

Mahowald, A. 1972. Ultrastructural observations on oogenesis in Drosophila. J. Morph. 137, 29-48.

Mazia, D., G. Schatten and W. Sale. 1975. Adhesion of cells to surfaces coated with poly-lysine. J. Cell Biol. 66, 198-200.

McGwin, N., R. Morton, and D. Nishioka. 1983. Increased uptake of thymidine in activation of sea urchin eggs. Exp. Cell. Res. 145, 115-126.

Moon, R., R. Nicosia, C. Olsen, M. Hille and W. Jeffery. 1983. The cytoskeletal framework of sea urchin eggs and embryos: developmental changes in the association of messenger RNA. Dev. Biol.

Mooseker, M. 1983. Actin binding proteins of the brush border. Cell. 35, 11-13.

Morrill, J. and F. Perkins. 1973. Microtubules in the cortical region of the Lymnaea egg during cortical segregation. Dev. Biol. 33, 206-212.

O'Donnel, M. 1986. Action potentials in Rhodnius oocytes: repolarization sensitive to potassium channel blockers. J. Exp. Biol. 126, 119-132.

Osborn, M. and K. Weber. 1977. The microtrabecular lattice of the cytoplasmic ground substance: artifact or reality. J. Cell Biol. 82, 114-139.

Otto, J. and T. Schroeder. 1984a. Microtubules arrays in the cortex and near the germinal vesicle of immature starfish oocytes. Dev. Biol. 101, 274-281.

Otto, J. and T. Schroeder. 1984b. Assembly-disassembly of actin bundles in starfish oocytes: an analysis of actin-associated proteins in the isolated cortex. Dev. Biol. 101, 263-273.

Palecek, J., V. Habrova, J. Nedvidek and A. Romanivsky. 1985. Dynamics of tubulin structures in Xenopus laevis oogenesis. J. Embryol. Exp. Morph. 87, 75-86.

Pruss, R., R. Mirsky and M. Raff. 1981. All classes of intermediate filaments share a common antigenic determinant defined by a monoclonal antibody. Cell. 27, 419-428.

Raff, R., J. Brandis, L. Green J. Kaumeyer and E. Raff. 1975. Microtubules protein pools in early development. Annals New York Acad. Sci. 253, 304-317.

Raven, C. 1970. The cortical and subcortical cytoplasm of the Lymnaea egg. Int. Rev. Cytol. 28, 1-44.

Reynolds, E. 1969. The use of lead citrate at high pH as an electron opaque stain in electron microscopy. J. Cell Biol. 17, 208-212.

Rioux, L. and C. Giquaud. 1985. Actin paracrystalline sheets formed at the surface of positively charged liposomes. J. Ultrastruc. Res. 93, 42-49.

Sardet, C. 1984. The ultrastructure of the sea urchin egg cortex isolated before and after fertilization. Dev. Biol. 105, 196-210.

Sardet, C. and P. Chang. 1987. The egg cortex: from maturation through fertilization. Cell Differentiation. 21, 1-19.

Satoh, N. and T. Deno. 1980. Periodic appearance and disappearance of microvilli associated with cleavage cycles in egg of Ascidian Halocynthia rortzi. Dev. Biol. 102, 488-497.

Sawada, T. and K. Osnai. 1985. Distribution of actin filaments in fertilized eggs of Ciona intestinalis. Dev. Biol. 111, 260-265.

Schatten, G. 1982. Motility during fertilization. Int. Rev. Cytol. 79, 59-163.

Schatten, G. and H. Schatten. 1983. Fertilization and early development of sea urchins. Scanning EM III, 1403-1413.

Schatten, H., M. Walter, D. Mazia, H. Biessmann, N. Paweletz, G. Coffe and G. Schatten. 1987. Centrosome detection in sea urchin eggs with a monoclonal antibody against Drosphila intermediate filament proteins: characterization of stages of the division cycle of centrosomes. Proc. Natl. Acad. Sci. USA. 75(4), 1820- 1824.

Schatten, G., T. Bestor, R. Balezon, J. Henson and H. Schatten. 1985. Intracelluar pH shift leads to microtubule assembly and microtubule mediated motility during sea urchin fertilization: correltaions between elevated intracellular pH and microtubule activity and depressed intracellular pH and microtubule disassembly. Eur. J. Cell Biol. 36, 116-127.

Schliwa, M. and J. Van Blerkon. 1981. Structural interaction of cytoskeletal components. J. Cell. Biol. 90, 222-235.

Schreiner, B. 1977. Vitellogenesis in the milkweed bug, Oncopeltus fasciatus Dallas (hemiptera). A light and electron microscope investigation. J. Morph. 151, 35-79.

Schroeder, T. 1972. The contractile ring II Determining its brief existence, volumetric changes and vital role in cleaving Arbacia eggs. J. Cell Biol.53, 419-434.

Schroeder, T. 1973. Actin in dividing cell: contractile ring filaments bind heavy meromyosin. Proc. Natl. Acad. Sci. USA. 70(6), 1688-1692.

Schroeder, T. 1982. Novel surface specialization on a sea anemone egg: "spires" of actin filled microvilli. J. Morph. 174, 207-216.

Schroeder, T. and J. Otto. 1984. Cyclic assembly-disassembly of cortical microtubules during maturation and early development of starfish oocytes. Dev. Biol. 103, 493-503.

Schroeder, T. and S. Stricker. 1983. Morphological changes during maturation of starfish oocytes: surface ultrastructure and cortical actin. Dev. Biol. 98, 373-384.

Shagli, R. and D. Philips. 1980. Mechanics of sperm entry in cycling hamsters. J. Ultrastruct. Res. 71, 154-161.

Shimizu, T. 1981. Cortical differentiation of the animal pole during maturation division in fertilized eggs of Tubifex (Annelida, Oligochaeta). I Meiotic apparatus formation. Dev. Biol. 85, 65-76.

Shimizu, T. 1985. Movements of mitochondria associated with isolated egg cortex. Develop. Growth and Differ. 27(2), 149-154.

Shimizu, T. 1986. Bipolar segregation of mitochondria, actin network and surface in Tubifex egg: role of cortical polarity. Dev. Biol. 116, 241-251.

Shimizu, T. 1988. Localization of actin networks during early development of Tubifex embryos. Dev. Biol. 125, 321-331.

Speksnijder, J., K. deJong, W. Linnemans and R. Dohmen. 1986. The organization of microfilaments, microtubules and clathrin coats in the cortex of molluscan eggs: temporal and spatial aspects. from J. Speksnijder. Ph.D. Thesis.

Spudich, A. and J. Spudich. 1979. Actin in triton-treated cortical preparations in unfertilized and fertilized sea urchin eggs. J. Cell Biol. 82, 212-226.

Spudich, J. and L. Amos. 1979. Structure of actin filament bundles from microvilli of sea urchin eggs. J. Mol. Biol. 129, 319-331.

Stebbings, H. 1986. Transport in cells: Movement and microtubules. Science News (Spectrum) 203, 2-4.

Steinert, R., J. Jones and R. Goldman. 1984. Intermediate filaments. J. Cell Biol. 99(1), 22s-27s.

Stossell, T. 1984. Contribution of actin to the structure of the cytoplasmic matrix. J. Cell Biol. 99(1), 15s-21s.

Telfer, W. 1975. Development and physiology of the oocyte-nurse cell syncytium. Adv. Insect Physiol. 11, 223-319.

Telfer, W. and E. Anderson. 1968. Functional transformations accompanying the initiation of a terminal growth phase in Cecropia moth oocytes. Dev. Biol. 17, 512-535.

Telfer, W., E. Huebner, and D. Smith. 1982. The cell biology of vitellogenic follicles in Hyalophora and Rhodnius. In Insect Ultrastructure Vol. 1. R.C King and H, Akai. (Eds). Plenum Press. New York. pp.118-149.

Tucker, J. 1981. Cytoskeletal coordination and intercellular signalling during metazoan embryogenesis. J. Embryol. Exp. Morph. 65, 1-25.

Tucker, J and M. Meats. 1976. Microtubules and control of insect egg shape. J. Cell. Bibl. 74, 207-217.

Vacquier, V. 1981. Dynamic changes of the egg cortex. Dev. Biol. 84, 1-26.

Valdimarsson, G. and E. Huebner. 1989. Diethylene glycol distearate as an embedding medium for immunofluorescence microscopy. In Press. Biochem. and Cell Biol.

Vanderberg, J. 1963. Synthesis and transfer of DNA, RNA and protein during vitellogenesis in Rhodnius prolixus (Hemiptera). Biol. Bull. 125, 556-575.

Villa, L. and E. Patricola. 1987. A scanning electron microscope study of Ascidia malaca egg (Tunicate). Changes in the cell surface morphology at fertilization. Biol. Bull. 173, 355-366.

Virtanen, I., R. Badley, R. Paasivuo and V-P. Lehto. 1984. Distinct cytoskeletal domains revealed in sperm cells. J. Cell Biol. 99, 1083-1091.

Walter, M. and H, Biessman. 1984. Intermediate size filaments in Drosophila tissue culture cells. J. Cell Biol. 99, 1468-1477.

Wang, Y. and D.L. Taylor. 1979. Distribution of fluorescently labelled actin in living sea urchin eggs during early development. J. Cell Biol. 82, 672-679.

Warn, R. and R. MaGrath. 1983. F-actin distribution during the cellularization of the Drosophila embryo visualized with FL-phalloidin. Exp. Cell Res. 143, 103-114.

Warn, R., H. Gutzeit, L. Smith and A. Warn. 1985. F-actin rings are associated with the Drosphila egg chamber canals. Exp. Cell Res. 157, 355-363.

Watson, A. and E. Huebner. 1986. Modulation of cytoskeletal organization during insect follicle morphogenesis. Tissue and Cell. 18(5), 741-752.

Weber, K. and M. Osborn. 1979. Intracellular display of microtubular structures revealed by indirect immunofluorescence microscopy. In Microtubules. K. Roberts and J. Hyams (Eds) Academic Press. pp. 279-313.

Weber, K., P. Rathke, and M. Osborn. 1978. Cytoplasmic microtubular images in glutaraldehyde-fixed tissue culture cells by electron microscopy and by immunofluorescence microscopy. Proc. Natl. Acad. Sci. USA. 75(4), 1820-1824.

Weber, K., R. Pollack and T. Bibring. 1975. Antibody against tubulin: the specific visualization of cytoplasmic microtubules in tissue culture cells. Proc. Natl. Acad. Sci. USA. 72, 459-463.

Weeds, A. 1982. Actin-binding proteins- regulation of cell architecture and motility. Nature. 296, 811-815.

Went, D. 1978. Oocyte maturation without follicular epithelium alters egg shape in a dipteran insect. J. Exp. Zool. 205, 149-155.

Wilson, E.B. 1925. The cell in development and heredity. Garland Press. New York. 1232p.

Wolosowick, J. and K. Porter. 1979. The microtubule lattice of the cytoplasmic ground substance: artifact or reality. J. Cell Biol. 82, 114-139.

Yonemura, S. and S. Kinoshita. 1986. Actin filament organization in the sand dollar egg cortex. Dev. Biol. 115, 171-183.

Zissler, D. and K. Sander. 1982. The cytoplasmic architecture of the insect egg cell. In Insect Ultrastructure Vol. 1. R.C. King and H. Akai (Eds). Plenum Press. New York. pp. 189-221.

APPENDIX I

Ovarioles were desheathed in Rhodnius saline (Maddrell, 1969) followed by fixation for 0.5 hr at room temperature in Carnoy's fixative (60mL ethyl alcohol, 30mL chloroform and 10mL glacial acetic acid). Ovarioles were then rapidly dehydrated through an ascending series of ice-cold ethyl alcohol to absolute ethyl alcohol. Tissue was placed in 100% ethyl alcohol for four 15 min changes at room temperature. Samples were then treated to 2:1 and 1:2 mixtures of n-butyl alcohol and 100% ethyl alcohol for 15 min each. Tissue was equilibrated in n-butyl alcohol for four 15 min changes. The ovarioles were then infiltrated in a 2:1 followed by a 1:2 mixture of n-butyl alcohol and DGD plus 0.5% DMSO at 55-60°C for 10 min each. Samples were placed in pure DGD with 0.5% DMSO at 55-60°C overnight. Next morning were placed in fresh DGD with 0.5% DMSO for 1 hr at 55-60°C, then embedded in Micron molds.

Sections, 1uM, were cut with glass knives at 4° angle on a Sorvall Porter-Blum MT2-B Ultramicrotome. They were floated onto subbed glass slides and left to air dry. Slides were stored in a dust free container until further use.

DGD was removed as per immunofluorescence- excluding $NaBH_4$ treatment, and the three minute times were increased to 10 min and slides were subjected to three 10 min changes in

100% ethyl alcohol. Sections were then rehydrated, using 10 min changes to deionized distilled water. Slides were then washed in 100mM Tris, 3mM $MgCl_2$ (Buffer I) for 5 min. All slides were washed in 0.01M Tris, 200mM NaCl, 5mM $MgCl_2$ (Buffer II) for 5 min. Control slides were then incubated in pancreatic RNAase A (100ug/mL in 10mM Tris-Cl, pH 7.6, 10mM KCl, and 1mM $MgCl_2$) (TKM buffer) for 16 hr at 37°C. Slides were subsequently washed for 5 min in Buffer II.

All slides were hybridized to a ^{3}H-poly U probe (New England Nuclear). 30uL aliquots of 2 or 4uCi were added to each slide. Sections were then covered by an acid washed coverslip and incubated for 3-4 hr at 50°C in a moist environment (Hybridization buffer).

After hybridization slides were washed in Buffer II, followed by TKM buffer for 5 min. Sections were then exposed to pancreatic RNAase A (50ug/mL in TKM buffer) for 1 hr at 37°C. Sections were washed again in TKM buffer for 5 min and washed rapidly in deionized distilled water. Treatment with ice-cold 5% TCA (tri-chloro-acetic acid) for 15 min preceded three rapid washes in deionized distilled water. Sections were then dehydrated in 70% ethyl alcohol/0.3M ammonium acetate, and 95% ethyl alcohol/0.3M ammonium acetate for two 5 min changes each. The slides were then air dried.

Slides were coated in a 1:1 mixture of ammonium acetate and Kodak autoradiography emulsion in the dark at 45°C, then left to air dry for 30 min at room temperature in the dark. They were then placed in a light tight container moistened with 30% hydrogen peroxide for 2.5 hr. Slides were left to expose for 5 weeks in a light tight desiccator at 4°C.

Slides were developed in D-19 Kodak developer for 2.5 min at 15°C with constant agitation for the first 30 sec. Slides were then transferred to 2% acetic acid (in deionized distilled H_2O) at 15°C for 30sec, followed by 5 min in 30% sodium thiosulfate (Hypo) at 15°C. Slides were washed in deionized distilled water at 15°C for 15 min and then under cold running water for 30 min. Slides were left to dry overnight, then mounted in Permount. Sections were examined using a Zeiss Photomicroscope II, both under bright field and dark field. Sections were photographed using Kodak Technical Pan 2415 film, ASA 50.